5-2024

Biotinylated Protein Capture and Tween-20 Assisted Exosome Isolations via Capillary Chanelled Polymer Fiber

Md Khalid Bin Islam
mdkhali@clemson.edu

BIOTINYLATED PROTEIN CAPTURE AND TWEEN-20 ASSISTED EXOSOME ISOLATIONS VIA CAPILLARY CHANELLED POLYMER FIBER

A Thesis

Presented to

the Graduate School of

Clemson University

In Partial Fulfillment

of the Requirements for the Degree

Master of Science

Chemistry

By Md Khalid Bin Islam

May 2024

Committee Members:

Dr. R. Kenneth Marcus, Committee Chair

Dr. Terri F. Bruce

Dr. Carlos D. Garcia

Dr. Daniel Whitehead

ABSTRACT

In the past two decades, Marcus and colleagues have led the advancement of capillary-channeled polymer (C-CP) fiber stationary phases for biomacromolecule separations, including proteins and nanovesicles. These stationary phases offer notable advantages, including low cost ($5/column), straightforward column fabrication, and the capacity for on-column surface modification, enabling high chemical selectivity. This study examines a C-CP fiber modification strategy for capturing target proteins and develops a Tween-20-assisted C-CP-based hydrophobic interaction chromatography (HIC) method for the isolation and quantification of exosomes from human urine.

The quest for higher-throughput and cost-effective protein isolation techniques remains a key focus in a variety of end uses. The streptavidin-biotin interaction, known for its exceptional specificity and stability, offers a promising avenue for protein purification. In this approach, immobilization of streptavidin (SAV) onto a solid substrate is crucial for the effective capture of biotinylated proteins. This study explores the potential of polypropylene (PP) C-CP fibers as support phases for SAV immobilization via direct adsorption. The PP C-CP fiber columns modified with SAV efficiently capture biotinylated proteins, indicating the promise of this approach for fast and cost-effective target protein capture.

Exosomes, membrane-secreted vesicles ranging from 30 to 200 nm, play crucial roles in intercellular communication and hold potential as therapeutic delivery vehicles. Efficient isolation and quantification methods are essential for studying their functions and therapeutic applications. Marcus and coworkers have developed Polyester (PET),

capillary-channeled polymer fiber columns, and spin-down tips as high-throughput and cost-effective approaches for exosome isolation. However, selecting the optimal elution solvent remains a challenge, particularly for preserving the structural integrity of the isolated vesicles. This study evaluates Tween-20, a non-ionic detergent, as an elution solvent for exosome recovery from human urine in advancing the versatility of C-CP fiber column-based HIC isolation methods.

DEDICATION

I dedicate this thesis to my beloved parents, whose unwavering love and support have been my guiding light throughout the highs and lows of pursuing this degree. To my wife, your encouragement and understanding have been my source of strength. And to all my friends in Clemson, your companionship has enriched this journey beyond measure.

ACKNOWLEDGMENTS

I extend my heartfelt gratitude to my dissertation committee members: Dr. Bruce, Dr. Whitehead, and Dr. Garcia, whose patience and belief in me have guided me through this journey. Special thanks are due to Dr. Marcus, whose unwavering commitment to pushing boundaries and fostering intellectual growth has significantly contributed to my development as a scientist. I deeply appreciate all my lab mates (past and present) whose help and support have been invaluable throughout this endeavor.

TABLE OF CONTENTS

LIST OF TABLES

LIST OF FIGURES

List of Figures (Continued)

CHAPTER ONE

INTRODUCTION

1.1 Protein Purification via Streptavidin-Biotin Interaction

Biotin labeling of target molecules in affinity chromatography presents versatile applications, including protein purification, antibody isolation, and bioconjugation methodologies.[1, 2] Streptavidin (SAV) serves as a prominent choice for the capture ligand in biotinylated protein purifications due to its remarkable affinity for biotin. The interaction between biotin and SAV is widely recognized as one of the strongest non-covalent interactions, characterized by an exceptionally low dissociation constant in the femto-molar range.[3] Biotin-labeled proteins using SAV-coupled resin provide excellent selectivity in the process. However, the choice of support resin is critical for SAV immobilization, requiring specificity to occur with minimal nonspecific binding. Over the years, various commercially available support phases have been developed to immobilize SAV which includes agarose, acrylamide, and sepharose-based supports, and SAV magnetic beads.[4, 5] However, the utilization of SAV support materials in large-scale protein purification poses a notable challenge due to their substantial cost implications. Therefore, a pressing demand exists for high-throughput, and cost-effective support matrices capable of affording substantial ligand binding capacity and maximal protein capture.

1.2 Capillary Channeled Polymer Fiber Stationary Phases

The efficacy of the capillary-channeled polymer (C-CP) fibers as a stationary phase for biomacromolecule separations including proteins and nanobodies has been demonstrated in previous studies by Marcus and colleagues.[6, 7] The C-CP fibers, extruded from commodity polymers of polypropylene (PP), polyester (PET), and nylon 6, offer a diverse spectrum of hydrophobicities and ionic characteristics, thereby facilitating chromatographic separation. Owing to the diverse array of surface chemistries available, C-CP fibers have been employed in a range of separation modalities, encompassing reversed phase (RP),[8] ion exchange (IEX),[9] affinity,[10] and hydrophobic interaction chromatography (HIC).[11] The enhancement of selectivity can be achieved by facile surface modifications of the fiber surfaces on-column using methods such as simple adsorption or covalent ligand coupling. The fiber structure is characterized by a distinctive cross-sectional profile featuring eight pronged shapes along the periphery. These fibers are virtually non-porous on the size scale of proteins and nanobodies.[12] While configured in a column format, thousands of 1 – 4 μm channels allow favorable mass transfer rates which facilitate faster protein capture.[7] Furthermore, C-CP fibers offer a cost-effective option, priced at approximately US $28/kg, in contrast to the minimal amount of support material, typically less than 1 g, utilized in a typical microbore column format (30 cm × 0.76 mm I.D.).

1.3 Modification of C-CP Fiber Surfaces for Protein Capture

Numerous studies have explored different ways to modify the surfaces of polymer fibers, as highlighted in literature.[13-15] However, it is important to consider that some of these modification methods could potentially harm the physical properties of the polymer,

such as degradation of its backbone.[13, 16] Therefore, it is crucial to find methods that enhance the fiber's chromatographic abilities while maintaining its structural integrity. To develop the protein capture selectivity utilizing C-CP fibers, there is a growing emphasis on exploring milder modification approaches. The interaction between macromolecules and the hydrophobic surface of PP C-CP fibers leads to physical adsorption, making these fibers a reliable support phase for immobilization. Past studies have examined various immobilization strategies on PP C-CP fibers, including using poly(ethylene glycol)-lipid and staphylococcal protein A to capture IgG.[17, 18] Focusing on gentler modification methods not only broadens the range of surface functionalization but also enhances the performance of C-CP fiber-based chromatographic systems by ensuring the durability of the polymer backbone, even after repeated cycles and integrity of the captured species for downstream analysis.

1.4 Isolation of Exosomes using Hydrophobic Interaction Chromatography

Exosomes, a subtype of extracellular vesicles (EVs), having sizes ranging from 30 – 200 nm are essential for intercellular communication.[19] Exosome possesses distinct surface biomarkers indicative of their cellular origin and offers potential as non-invasive biomarkers due to their stability and abundance in bodily fluids.[20] Exosomes are actively investigated for their role in targeted cargo delivery, with emerging applications in drug delivery and therapeutics.[21] As the field advances towards utilizing exosomes for diagnostics and therapeutics, there is a pressing need for efficient methods for exosome isolation and quantification.

Marcus and coworkers have developed polyester (PET), C-CP fiber based HIC methodology to isolate and quantify exosomes from complex biological matrices.[22] This

methodology has demonstrated efficacy in the successful isolation of exosomes from diverse complex biofluids, including urine, saliva, blood serum, cervical mucus, cell culture media, and plant samples.[22-24] While having a similar retention mechanism with RP-LC, a primary advantage of HIC lies in the milder interactions between analytes and the stationary phase. In HIC, a gradient of salt concentration is utilized, transitioning from high to low levels, to facilitate the elution of the molecules (ionic species, proteins etc.) in order of increasing hydrophobicity.[11, 22] Organic solvent modifiers such as acetonitrile (ACN), glycerol, or Tween-20 are utilized for the eventual elution of exosomes. A commonly implemented exosome elution sequence involves a step gradient where the salt content is reduced to zero, and the organic modifier solution concentration is increased to 40–50% in PBS. The modulation of retention and selectivity in C-CP based HIC can be achieved through elution solvent choice towards specific end-uses such as fundamental biochemistry, clinical diagnostics, or therapeutic vectors.

1.5 Solvent Modifier in HIC Methodology

The exploration of solvent modifiers in HIC based exosome isolation methods can provide valuable insights into tailoring strategies for specific downstream applications while maximizing yield and minimizing potential interference in subsequent analyses. In the context of exosome separation using HIC on C-CP platform, elution solvents incorporating organic solvents (ACN and glycerol) and non-ionic detergent Tween-20 have been explored, each potentially offering distinct advantages depending on the intended downstream application of the eluted vesicles.[22, 25, 26] Glycerol, a common modifier, is favored in situations where the long-term stability of the vesicles is a priority. However, the use of glycerol as a solvent modifier comes with drawbacks, including its

tendency to inhibit surface marker affinity interactions, high viscosity, and the neutralization of the vesicles' surface charge—factors that can adversely affect various immunoaffinity-based applications.[27, 28] ACN causes less interference in affinity-based characterization analyses and can be removed by off-gassing. However, it is essential to note that ACN may not be ideal for applications involving cell uptake, as high concentrations of ACN are known to be toxic to cells.[29] As an alternative approach a non-ionic detergent, Tween-20 as an elution solvent was explored by this group to isolate exosomes from human embryonic kidney cells.[26] However, Increased concentrations of Tween-20 may present limitations for specific applications, notably in mass spectrometry proteomic workflows.[30] Thus, a thorough investigation into the suitability of Tween-20 as an elution solvent is required, aiming to optimize high-throughput isolation while ensuring the preservation of structural integrity of the vesicles.

1.6 References

(1) de Boer, E.; Rodriguez, P.; Bonte, E.; Krijgsveld, J.; Katsantoni, E.; Heck, A.; Grosveld, F.; Strouboulis, J. Efficient biotinylation and single-step purification of tagged transcription factors in mammalian cells and transgenic mice. *PNAS* **2003**, *100* (13), 7480-7485.

(2) Aissa, A. B.; Herrera-Chacon, A.; Pupin, R.; Sotomayor, M.; Pividori, M. Magnetic molecularly imprinted polymer for the isolation and detection of biotin and biotinylated biomolecules. *Biosens. Bioelectron.* **2017**, *88*, 101-108.

(3) Green, N. M. [5] Avidin and streptavidin. In *Methods Enzymol.*, Vol. 184; Elsevier, 1990; pp 51-67.

(4) Wollscheid, B.; Bausch-Fluck, D.; Henderson, C.; O'brien, R.; Bibel, M.; Schiess, R.; Aebersold, R.; Watts, J. D. Mass-spectrometric identification and relative quantification of N-linked cell surface glycoproteins. *Nat. Biotechnol.* **2009**, *27* (4), 378-386.

(5) Haukanes, B.-I.; Kvam, C. Application of magnetic beads in bioassays. *Biotechnol.* **1993**, *11* (1), 60-63.

(6) Marcus, R. K.; Davis, W. C.; Knippel, B. C.; LaMotte, L.; Hill, T. A.; Perahia, D.; Jenkins, J. D. Capillary-channeled polymer fibers as stationary phases in liquid chromatography separations. *J. Chromatogr. A* **2003**, *986* (1), 17-31.

(7) Nelson, D. M.; Marcus, R. K. Characterization of capillary-channeled polymer fiber stationary phases for high-performance liquid chromatography protein separations: comparative analysis with a packed-bed column. *Anal. Chem.* **2006**, *78* (24), 8462-8471.

(8) Randunu, K. M.; Marcus, R. K. Microbore polypropylene capillary channeled polymer (C-CP) fiber columns for rapid reversed-phase HPLC of proteins. *Anal. Bioanal. Chem.* **2012**, *404*, 721-729.

(9) Jiang, L.; Marcus, R. K. Microwave-assisted, grafting polymerization preparation of strong cation exchange nylon 6 capillary-channeled polymer fibers and their chromatographic properties. *Anal. Chim. Acta.* **2017**, *977*, 52-64.

(10) Schadock-Hewitt, A. J.; Marcus, R. K. Initial evaluation of protein A modified capillary-channeled polymer fibers for the capture and recovery of immunoglobulin G. *J. Sep. Sci.* **2014**, *37* (5), 495-504.

(11) Stanelle, R. D.; Marcus, R. K. Nylon-6 capillary-channeled polymer (C-CP) fibers as a hydrophobic interaction chromatography stationary phase for the separation of proteins. *Anal. Bioanal. Chem.* **2009**, *393*, 273-281.

(12) Wang, Z.; Marcus, R. K. Determination of pore size distributions in capillary-channeled polymer fiber stationary phases by inverse size-exclusion chromatography and implications for fast protein separations. *J. Chromatogr. A* **2014**, *1351*, 82-89.

(13) Farrow, G.; Ravens, D.; Ward, I. The degradation of polyethylene terephthalate by methylamine—A study by infra-red and X-ray methods. *Polym.* **1962**, *3*, 17-25.

(14) Zahn, H.; Pfeifer, H. Aminolysis of polyethylene terephthalate. *Polymer* **1963**, *4*, 429-432.

(15) Avny, Y.; Rebenfeld, L. Chemical modification of polyester fiber surfaces by amination reactions with multifunctional amines. *J. Appl. Polym. Sci.* **1986**, *32* (3), 4009-4025.

(16) Ellison, M.; Fisher, L.; Alger, K.; Zeronian, S. Physical properties of polyester fibers degraded by aminolysis and by alkalin hydrolysis. *J. Appl. Polym. Sci.* **1982**, *27* (1), 247-257.

(17) Trang, H. K.; Schadock-Hewitt, A. J.; Jiang, L.; Marcus, R. K. Evaluation of loading characteristics and IgG binding performance of Staphylococcal protein A on polypropylene capillary-channeled polymer fibers. *J. Chromatogr. B* **2016**, *1015*, 92-104.

(18) Schadock-Hewitt, A. J.; Marcus, R. K. Loading characteristics and chemical stability of headgroup-functionalized poly (ethylene glycol)-lipid ligand tethers on polypropylene capillary-channeled polymer fibers. *J. Sep. Sci.* **2014**, *37* (24), 3595-3602.

(19) Simons, M.; Raposo, G. Exosomes–vesicular carriers for intercellular communication. *Curr. Opin. Cell Biol.* **2009**, *21* (4), 575-581.

(20) Kalishwaralal, K.; Kwon, W. Y.; Park, K. S. Exosomes for non-invasive cancer monitoring. *Biotechnol. J.* **2019**, *14* (1), 1800430.

(21) Liang, Y.; Duan, L.; Lu, J.; Xia, J. Engineering exosomes for targeted drug delivery. *Theranostics* **2021**, *11* (7), 3183.

(22) Bruce, T. F.; Slonecki, T. J.; Wang, L.; Huang, S.; Powell, R. R.; Marcus, R. K. Exosome isolation and purification via hydrophobic interaction chromatography using a polyester, capillary-channeled polymer fiber phase. *Electrophoresis* **2019**, *40* (4), 571-581.

(23) Jackson, K. K.; Powell, R. R.; Bruce, T. F.; Marcus, R. K. Rapid isolation of extracellular vesicles from diverse biofluid matrices via capillary-channeled polymer fiber solid-phase extraction micropipette tips. *Analyst* **2021**, *146* (13), 4314-4325.

(24) Jackson, K. K.; Mata, C.; Marcus, R. K. A rapid capillary-channeled polymer (C-CP) fiber spin-down tip approach for the isolation of plant-derived extracellular vesicles (PDEVs) from 20 common fruit and vegetable sources. *Talanta* **2023**, *252*, 123779.

(25) Huang, S.; Wang, L.; Bruce, T. F.; Marcus, R. K. Evaluation of exosome loading characteristics in their purification via a glycerol-assisted hydrophobic interaction chromatography method on a polyester, capillary-channeled polymer fiber phase. *Biotechnol. Prog.* **2020**, *36* (5), e2998.

(26) Jackson, K. K.; Marcus, R. K. Rapid isolation and quantification of extracellular vesicles from suspension-adapted human embryonic kidney cells using capillary-channeled polymer fiber spin-down tips. *Electrophoresis* **2023**, *44* (1-2), 190-202.

(27) Vagenende, V.; Yap, M. G.; Trout, B. L. Mechanisms of protein stabilization and prevention of protein aggregation by glycerol. *Biochemistry* **2009**, *48* (46), 11084-11096.

(28) Vagenende, V.; Trout, B. L. Quantitative characterization of local protein solvation to predict solvent effects on protein structure. *Biophys. J.* **2012**, *103* (6), 1354-1362.

(29) Zabrodsky, P. Acetonitrile intoxication impact on humoral and cellular immune responses. *J. Cardiol. Curr. Res* **2019**, *12*, 78-80.

(30) Heller, N. C.; Garrett, A. M.; Merkley, E. D.; Cendrowski, S. R.; Melville, A. M.; Arce, J. S.; Jenson, S. C.; Wahl, K. L.; Jarman, K. H. Probabilistic limit of detection for ricin identification using a shotgun proteomics assay. *Anal. Chem.* **2019**, *91* (19), 12399-12406.

1.7 Summary of Chapters

CHAPTER TWO

LOADING CHARACTERISTICS OF STREPTAVIDIN ON POLYPROPYLENE CAPILLARY CHANNELED POLYMER FIBERS AND CAPTURE PERFORMANCE TOWARDS BIOTINYLATED PROTEINS

The development of higher throughput, potentially lower cost means to isolate proteins, for a variety of end uses, is of continuing emphasis. Polypropylene (PP) capillary-channeled polymer (C-CP) fiber columns are modified with the biotin-binding protein streptavidin (SAV) to capture biotinylated proteins. The loading characteristics of SAV on fiber supports were determined using breakthrough curves and frontal analysis. Based on adsorption data, a 3 min on-column loading at a flow rate of 0.5 mL min^{-1} (295.2 cm h^{-1}) with a 0.5 mg mL^{-1} SAV feed concentration, produces an SAV loading capacity of 1.4 mg g^{-1} fiber. SAV has an incredibly high affinity for the small molecule biotin (10^{-14} M), such that this binding relationship can be exploited by labeling a target protein with biotin via an Avi-tag. To evaluate the capture of the biotinylated proteins on the modified PP surface, the biotinylated versions of bovine serum albumin (b-BSA) and green fluorescent protein (b-GFP) were utilized as probe species. The loading buffer composition and flow rate were optimized towards protein capture. The non-ionic detergent Tween-20 was

added to the deposition solutions to minimize non-specific binding. Values of 0.25 - 0.50% (v/v) Tween-20 in PBS exhibited better capture efficiency, while minimizing the non-specific binding for b-BSA and b-GFP, respectively. The C-CP fiber platform has the potential to provide a fast and low-cost method to capture targeted proteins for applications including protein purification or pull-down assays.

CHAPTER THREE

ISOLATION AND QUANTIFICATION OF HUMAN URINARY EXOSOMES USING A TWEEN-20 ELUTION SOLVENT FROM POLYESTER, CAPILLARY-CHANNELED POLYMER FIBER COLUMNS

Exosomes, a subset of extracellular vesicles (EVs) are a type of membrane-secreted vesicle essential for intercellular communication. There is a great deal of interest in developing methods to isolate and quantify exosomes to study their role in intercellular processes and as potential therapeutic delivery systems. Polyester, capillary-channeled polymer fiber columns and spin-down tips are highly efficient, low-cost means of exosome isolation. As the methodology evolves, there remain questions as to the optimum elution solvent for specific end-uses of the recovered vesicles; fundamental biochemistry, clinical diagnostics, or therapeutic vectors. While both acetonitrile and glycerol have been proven highly successful in terms of EV recoveries in the hydrophobic interaction chromatography workflow, many biological studies entail the use of the non-ionic detergent, Tween-20, as a working solvent. Here we evaluate the use Tween-20 as the elution solvent for the recovery of exosomes. A novel 10-minute, two-step gradient elution

method, employing 0.1% v/v Tween-20, efficiently isolated EVs at a concentration of ~10^{11} EVs mL^{-1} from a 100 µL urine injection. Integration of absorbance and multi-angle light scattering detectors in standard HPLC instrumentation enables a comprehensive single-injection determination of eluted exosome concentration and sizes. Transmission electron microscopy verifies the retention of the vesicular structure of the exosomes. The micro-bicinchoninic acid protein quantification assay confirmed high-purity (~ 99%) isolations of EVs from background proteins. The effective use of Tween-20 as an elution solvent for exosome isolation/purification using capillary-channeled polymer fiber columns adds greater versatility to the portfolio of the approach. The proposed method holds promise for a wide range of fundamental biochemistry, clinical diagnostics, and therapeutic applications, marking a significant advancement in EV-based methodologies.

1.8 List of Publications

The following chapters in this dissertation are based on these papers:

Chapter Two: Islam, M.K.B.; Marcus, R.K. Loading Characteristics of Streptavidin on Polypropylene Capillary Channeled Polymer Fibers and Capture Performance towards Biotinylated Proteins. *Analytical and Bioanalytical Chemistry* **2023**, *415* (27), 6711–6721.

Chapter Three: Islam, M.K.B.; Marcus, R.K. Isolation and Quantification of Human Urinary Exosomes Using a Tween-20 Elution Solvent from Polyester, Capillary-Channeled Polymer Fiber Columns. *Analytica Chimica Acta* **2024**, *(submitted for publication)*.

CHAPTER TWO

LOADING CHARACTERISTICS OF STREPTAVIDIN ON POLYPROPYLENE CAPILLARY CHANNELED POLYMER FIBERS AND CAPTURE PERFORMANCE TOWARDS BIOTINYLATED PROTEINS

2.1 Introduction

Purification of proteins and antibodies from complex biological samples has grown as a key process in the biotechnology and pharmaceutical industries, offering diverse applications in diagnostics, therapeutics, and fundamental biochemical research.[1-3] A wide range of innovative uses, including recombinant protein therapies, monoclonal antibody-based treatments, and the emergence of personalized medicine, have fueled the development of new separation technologies.[4, 5] The escalating need for proteins and antibodies for diverse applications has catalyzed the expansion of the global chromatography market. As of 2020, the market for chromatography resins has exceeded a value of 6.0 billion USD.[6] To address the issues of purifying specific targets, new ligands and resin materials have been introduced to improve separation efficiency. Significant progress has been achieved in the development of affinity-based enrichment methodologies during the last few decades, particularly in the areas of ligand discovery, resin development, and process optimization.[7, 8]

Affinity-based purification relies on the specific binding of the target molecule to a ligand immobilized on a solid support. Biotin-tagging of target molecules has widespread applications in protein purification, antibody isolation, and bioconjugation techniques.[9, 10] Due to its extremely high affinity for biotin, streptavidin (SAV) is widely used as the capture ligand in the case of biotinylated protein purifications. With a dissociation constant (K_D) of 10^{-14} M, the streptavidin-biotin interaction is considered as one of the strongest non-

covalent interactions known, allowing for highly specific and stable binding.[11] Because of the low contributions to further non-specific binding and coincident rapid binding kinetics, the streptavidin-biotin interaction is a highly efficient approach for purifying biomolecules. This methodology has been used for a variety of purposes, including target protein purification, proteomics, protein pull-down assays, and the investigation of protein-protein interactions.[12, 13] However, even with such a strong interaction of the streptavidin-biotin complex, non-specific binding can occur, most commonly with the support material, resulting in lower target protein purity and yield.[14] The choice of solid support, thus has aspects of surface coverage, non-specific binding, mass transfer kinetics, processibility, and ultimately cost.

A crucial step in the effective application of streptavidin-biotin affinity chromatography for the purification of proteins and antibodies is the immobilization of SAV onto a solid substrate. For SAV immobilization, a number of commercially available support phases have been developed over the years. Agarose, acrylamide, and sepharose-based support phases have been reported in ligand receptor and cell surface protein capture studies.[15, 16] Agarose, with its large pore size and low non-specific binding, is a popular choice in affinity chromatography. However, agarose support phases have limitations regarding low mechanical stability at high operating pressures in the high-performance liquid chromatography (HPLC) systems.[17] Streptavidin-coated magnetic beads are another viable support phase, allowing rapid initial capture from bulk solution and particle isolation via application of a simple magnetic field.[18] The magnetic beads have an iron oxide layer which can be functionalized with a ligand that binds streptavidin capture ligand. Various streptavidin magnetic bead products have been described for use

in proteomic workflows.[19-21] Several benefits of magnetic beads include their high binding capacity and rapid kinetics. Nevertheless, magnetic beads can suffer from aggregation,[22] leading to reduced binding efficiency and increased nonspecific binding. Finally, use of streptavidin beads in large-scale protein purification presents a considerable hurdle due to their high cost.

In general, reliable, stable, high throughput, and cost-effective supports that can deliver high ligand binding capacity and maximum protein capture are needed across the protein purification and diagnostics space. Marcus et al. have demonstrated the use of capillary-channeled polymer (C-CP) fibers as stationary phases for the isolation and purification of proteins [23-25] and of bionanovesicles including exosomes and virus particles.[25-27] C-CP fibers can be extruded from base polymers of nylon-6, polypropylene, and polyester, presenting a range of surface hydrophobicities, ionic character, and functionality. The fiber phases have been employed both in standard HPLC column and spin-down tip formats [28-30] with the latter allowing for rapid throughput and parallel processing. A number of relatively simple fiber surface modifications have been implemented to affect protein separation selectivity including amination,[31] carboxylation [32] and biotinylation.[33] Interactions between macromolecules and the very hydrophobic polypropylene (PP) C-CP fiber surface result in physical adsorption. This phenomenon has led to the application of these fibers as a support phase for the robust immobilization of protein A and achieving immunoglobulin G (IgG)-specific capture both in the column and spin-down tip formats.[34-36]

Beyond their chemical characteristics towards affecting separations, C-CP fibers possess a distinct characteristic in the form of eight capillary channels that extend along

their length. These capillary channels exhibit interdigitating properties, enabling the formation of well-aligned micrometer-sized channels when the fibers are packed into a column format.[23, 37] This unique shape allows for high volume flow rates (1 mL min^{-1}) with low back pressure (<250 psi). Very favorable mass transfer rates are possible due to the non-porous surface of the C-CP fibers which facilitates faster protein capture.[38,39] Moreover, C-CP fibers are fairly inexpensive (~ \$28 kg^{-1}), whereas a typical microbore column is composed of <1 g of support material.

In this study, the potential of PP C-CP fibers as support phases for the immobilization of SAV through direct adsorption is explored as a means to capture specific biotinylated target proteins. To achieve this, the C-CP fiber packed microbore column format was employed on an HPLC system. Frontal analysis was performed on columns at different ligand concentration levels and volumetric flow rates to determine the dynamic loading characteristics of SAV on the PP C-CP fibers. These results provide the optimal loading conditions for generating the SAV-modified protein capture columns. In the second part of the study, the capture efficiency of biotinylated bovine serum albumin (b-BSA) with a fluorescent tag and a biotinylated green fluorescent protein (b-GFP) was evaluated using the UV-Vis absorbance and fluorescent detectors. Optimization of the protein loading conditions (e.g. flow rate and solvent composition) was undertaken to evaluate the balance between targeted protein capture and minimization of non-specific binding. It is believed that the C-CP fiber surface will evolve as an efficient and cost-effective platform for targeted (biotinylated) protein capture, including preparative column formats, as well as spin-down tips applicable for high-throughput pull-down assays.

2.2 Materials and Methods

2.2.1 Chemicals and solution preparation -

Deionized (DI) water was obtained from a milli-Q purification system (18.2 MΩ-cm, purified with Millipore, Merck, Germany). Gibco phosphate buffered solution (PBS) 10X pH 7.4 (ThermoScientific, MA, USA) was diluted in DI water to prepare 1X solution which was used as a stock PBS for further materials dilutions. Bovine serum albumin (BSA) (Sigma Aldrich, St. Louis, MO) was prepared as a stock solution at a concentration of 2 mg mL^{-1} in PBS. A 1% (v/v) solution of Tween-20 (VWR, Solon, OH, USA) in PBS was prepared as a stock Tween-20 solution. Streptavidin, biotinylated BSA (b-BSA) with a fluorescein fluorescent tag, green fluorescent protein (GFP) and biotinylated GFP (b-GFP) were all obtained from Integrated Micro-Chromatography System (IMCS) (Columbia, SC, USA) in bulk stock solutions of concentrations of 2.8, 3.11, 1.73, and 1.80 mg mL^{-1}, respectively. All further dilutions were prepared in PBS from the stock solutions. HPLC grade acetonitrile (ACN) (VWR, PA, USA) was used for cleaning and washing columns.

2.2.2 C-CP fiber column construction and instrumentation -

The methodology employed for packing C-CP fibers into PEEK microbore (0.76 mm, i.d.) columns has been previously described.[28, 35] A similar method was used here to pack PP C-CP fibers into a 2.4 mm i.d., 30 cm long PEEK tubing (Trajan Scientific and Medical, USA), as an extension of the method to a pneumatically-actuated pull down tip is ultimately envisioned. To ensure low solution flow resistance, a total of 2880 PP fibers were pulled through the column. After the fiber-packed columns were prepared, ACN and DI-H_2O were flushed through at a flow rate of 1 mL min^{-1} using the HPLC system.

The flushing continued until a stable baseline was achieved as determined by the UV absorbance detector at 216 nm. To assess the packing uniformity of the constructed fiber columns, the interstitial fraction (ε_i) was determined using uracil retention. The calculated interstitial fraction for all the columns was found to be 0.78, with less than 4% variability, which ensured the consistency and packing uniformity of the constructed columns. Once the stability was confirmed, each column was precisely cut into 10 cm lengths with each column containing an average of 0.3582 g of fiber material. The cleaning and chromatographic experiments were performed using a Dionex Ultimate 3000 HPLC system controlled by Chromeleon 7.0 software. The system consisted of an LPG-3400SD pump, a WPS-3000TSL autosampler, a VWD-3400RS UV–vis absorbance detector, and a VWD FLD detector.

2.2.3 Loading process and dynamic binding capacity of SAV column –

The methodology to affect an SAV capture column towards biotinylated proteins follows directly from the method originally developed to immobilize protein A onto PP fibers for IgG capture.[34-36] The loading process and dynamic binding capacity (DBC) of SAV on PP C-CP fiber column were measured by breakthrough curves and frontal analysis. To immobilize SAV onto the PP C-CP fibers, a simple adsorption process was employed, where 0.5 mg mL^{-1} SAV in PBS buffer was passed through the column until a plateau in the absorbance response was reached indicating surface saturation (3 min) as depicted in Fig. 1.

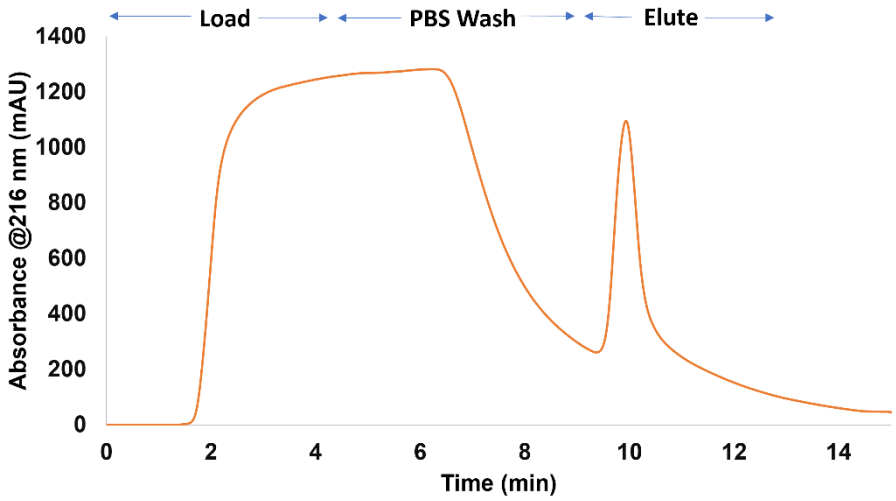

Fig. 2.1 Response for the load and elution steps of SAV on 10-cm C-CP fiber packed column. Loading solution: 0.5 mg mL^{-1} SAV, flow rate: 0.5 mL min^{-1}

As the solution passes over the fiber surfaces, SAV is continuously adsorbed to the surface until the surface sites became saturated, and SAV is no longer retained. At this point, the optical absorbance dramatically increases to a value equal to that of an ambient SAV solution. The DBC_{50} was calculated based on the SAV feed concentration, flow rate, and loading time.[38] The loading time was taken as the time to reach 50% of feed concentration (termed DBC_{50}) based on the measured optical absorbance values at 216 nm. The loading step was followed by a PBS wash step to return the absorbance to the background level. As a confirmation of the load amount, an elution step with 40% (v/v) ACN in PBS was applied to elute-off the retained SAV from the fiber column. If desired, a given PP fiber column could be re-used through the complete process, stripping the fiber surface of the adsorbed SAV as indicated by the return of the absorbance to background levels. Exposure of the PP fibers to such concentrations of ACN is in fact not deleterious to the virtually chemically-inert olefinic surface as demonstrated in repeated uses of PP C-CP fiber columns in reversed-phase protein separations.[40]

Likewise, this means of elution points to the hydrophobic nature of the streptavidin-PP fiber surface interaction. (Note that the same approach could, in principle, be used to harvest captured proteins from the capture column with the biotin/SAV complex remaining intact.) Frontal analysis was performed at a constant flow rate of 0.5 mL min^{-1} through the 10-cm long fiber columns at SAV feed concentrations of 0.05, 0.1, 0.3, 0.5, 0.7, 0.9, and 1.0 mg mL^{-1}. Additionally, the effect of volume flow rates on the loading of SAV was evaluated by passing a 0.5 mg mL^{-1} solution at 0.1, 0.3, 0.5, 0.7, 0.9, and 1.0 mL min^{-1}, corresponding to linear velocities of 57.6, 176.4, 295.2, 414, 532.8, and 590.4 cm h^{-1}, respectively.

2.2.4 Binding characteristics of biotinylated proteins on adsorbed SAV -

Following the parametric optimization, the SAV-modified column was prepared by loading SAV in a PP packed 10-cm column at a flow rate of 0.5 mL min^{-1} (295.2 cm h^{-1}) with a 0.5 mg mL^{-1} feed concentration for 3 min. The aim of monitoring protein binding performance on the modified column was to maximize target species capture while minimizing non-specific binding to ensure a selective protein capture strategy. The specific binding of the SAV-modified PP surface was assessed using two biotinylated proteins; biotinylated BSA (b-BSA) with a fluorescence tag and biotinylated GFP (b-GFP). The concept utilized in this system is illustrated in Fig. 2. The integrated elution peak area reflects the unretained biotinylated proteins with the following conditions – no column in-line and SAV-modified column in-line. The fraction of on-column unretained proteins was determined by taking the ratio of the peak area for the pass-through (un-retained) species to that obtained without a column. Considering the analytical signal that comes from the total pass through (total unretained species with no column in line) as 100%

protein amount injected, the retained amount of the modified column was computed. This parameter, referred to as "capture efficiency" in this study, quantifies the extent to which proteins are retained on the column, normalized to a scale of 100% capture. UV detection at 216 nm was utilized to measure b-BSA capture, and fluorescence excitation at 400 nm and emission at 510 nm were set to measure b-GFP capture. Non-specific binding on the modified surface was assessed from the native BSA and GFP injections. In each case, 4 µg of each of the respective proteins was injected onto the SAV-modified PP fiber column.

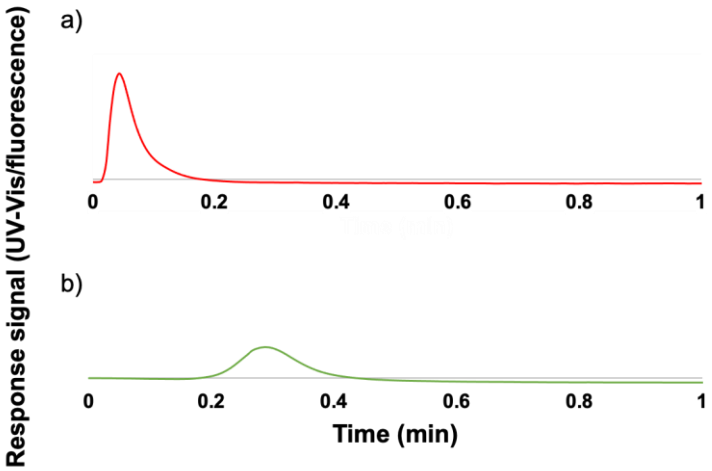

Fig. 2.2 Typical injection profile of biotinylated proteins with a) no column in-line, and b) SAV-modified column in-line

To assess the impact of flow rate on the binding of the b-BSA and b-GFP, the loading solvent buffer of 1X PBS introduced at volume flow rates of 0.3, 0.5, 0.7, and 0.9 mL min^{-1}, or a range of 176.4 – 590.4 cm h^{-1} (0.49 – 1.48 mm s^{-1}) in linear velocity. In order to assess and optimize the respective target protein capture while reducing non-specific binding, a systematic investigation of the loading buffer in the presence of the non-ionic detergent Tween-20 was evaluated. Tween-20 concentrations of 0.25%, 0.50%, 0.75%, and 1.0% in PBS (v/v) were explored. Both biotinylated proteins and their

native counterparts were injected into the system at a constant loading buffer flow rate of 0.5 mL min^{-1}.

2.2.5 Effects of background proteins -

To evaluate the effects of background proteins on the selective capture of the b-GFP, a protein mixture comprising both "soft" and "hard" proteins was prepared. The protein mixture consisted of four proteins with equal mass of ribonuclease A, lysozyme, thyroglobulin, and BSA. By utilizing this protein mixture, the study aimed to assess the impact of background proteins on the selective capture of b-GFP. The inclusion of both "soft" and "hard" proteins in the mixture allowed for a comprehensive evaluation of the binding behavior and selectivity under these conditions. The protein mixture was added to b-GFP to prepare the test separate protein mixture with equal mass ratio of the background and test proteins. A 4 µg protein mixture was injected (20 mL) at a constant flow rate of 0.5 mL min^{-1}. A loading solvent condition of 0.50% (v/v) Tween-20 in PBS was used as it was shown to result in the lowest amount of non-specific binding of GFP.

2.3 Results and Discussion

2.3.1 SAV loading characteristics -

Streptavidin monolayers are commonly used for immobilizing biotinylated proteins, receptors, and DNA due to their strong binding affinity for biotin.[41, 42] In this study, the immobilization of SAV onto the (PP) fibers is investigated through a simple adsorption process. Due to its nonpolar molecular structure, the highly hydrophobic nature of PP fibers dictates that the interaction between SAV and fibers is primarily hydrophobic, as was the case in the protein A and FITC-PEG lipids application.[34] The adsorption of SAV on a hydrophobic surface is typically observed to be irreversible under normal aqueous

buffer conditions.[43] The adsorptive ligand loading process here can potentially lead to improper orientation or random geometric orientation of the ligand molecules. Moreover, overloading of the substrate with the SAV capture ligand can lead to steric hindrance that negatively impacts the orientation and accessibility of binding sites, which in turn can affect the binding affinity and specificity towards the capture molecule. This issue is particularly concerning when working with proteins that possess multiple binding sites. As a result, either the support surface or the neighboring ligands can affect the specificity of the ligand.

To investigate the immobilization of SAV on PP fiber, dynamic binding characteristics were generated from a series of consecutive frontal analysis experiments. These experiments were conducted across a range of SAV input concentrations spanning from 0.05 to 1 mg mL^{-1}. Breakthrough curves were obtained in triplicate at a flow rate of 0.5 mL min^{-1} (295.2 cm h^{-1}). The determined dynamic binding capacities of SAV per mass fiber was plotted (as an adsorption isotherm) as a function of the solute concentration. Figure 3 shows that DBC_{50} values increased in a near-linear fashion with the solute

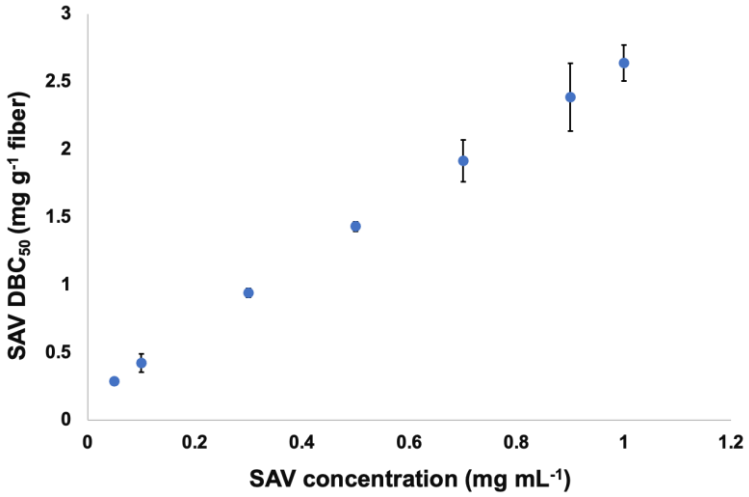

Fig. 2.3 Dynamic binding capacity (DBC_{50}) of SAV on PP C-CP fiber column at various feed concentrations.

concentration. The dynamic adsorption data was successfully fit to a linear model, yielding a correlation coefficient R_2 of 0.999. Utilizing MATLAB (MathWorks, Natick, MA, USA) software, the data were fit to Langmuir, Freundlich, and BET isotherm models [44]. The Langmuir model exhibited a fit with a correlation coefficient of 0.9945, with the Freundlich and BET models, designed for situations of multilayering or heterogeneous surface adsorption, yielding correlation coefficients of 0.9978 and 0.9984, respectively. Previous investigations have also unveiled similar close-to-linear isotherm trends in diverse adsorption scenarios on C-CP fibers, such as FITC-PEG lipids, staphylococcal protein A on PP fibers, and lysozyme/BSA on PET fibers.[35, 45, 46] It is pertinent to note that protein A adsorption onto PP fibers exhibited a mildly S-shaped isotherm. However, the linear isotherm behavior at lower SAV concentrations aligns well with the isotherm characteristics of FITC-PEG lipid adsorption on PP fibers. Ulitmately, the lack of "nonlinear" adsorption phenomena in the responses suggests the absence surface heterogeneity or multilayering.[47] Given the linear trend of the adsorption isotherm, it is plausible that the maximum capacity of the C-CP fiber column may not have been reached within the employed concentration range (0.05 – 1 mg mL^{-1} SAV). However, in order to assess the binding capacity of biotinylated proteins on the SAV-modified PP surface, a nominal feed concentration of 0.5 mg mL^{-1} was adopted. This concentration provides a reasonable level of SAV binding on the PP surface, yielding 1.4 mg g^{-1} SAV on the fiber surface (2.7×10^{-8} moles g^{-1} fiber) and well in the range of the linear binding data. Admittedly, this concentration likely represents a compromise in the absolute protein binding capacity, but sets a good level during these basic studies. Likewise, this implies that there is available fiber surface area wherein non-specific binding might occur.

One other consideration in the on-column loading procedure that can affect the ligand orientation and density is the loading flow rate. Optimization of the flow rate condition can lead to an optimum in mass transfer kinetics for a uniform immobilization on the fiber surface. Figure 4a represents the breakthrough curves across the variation

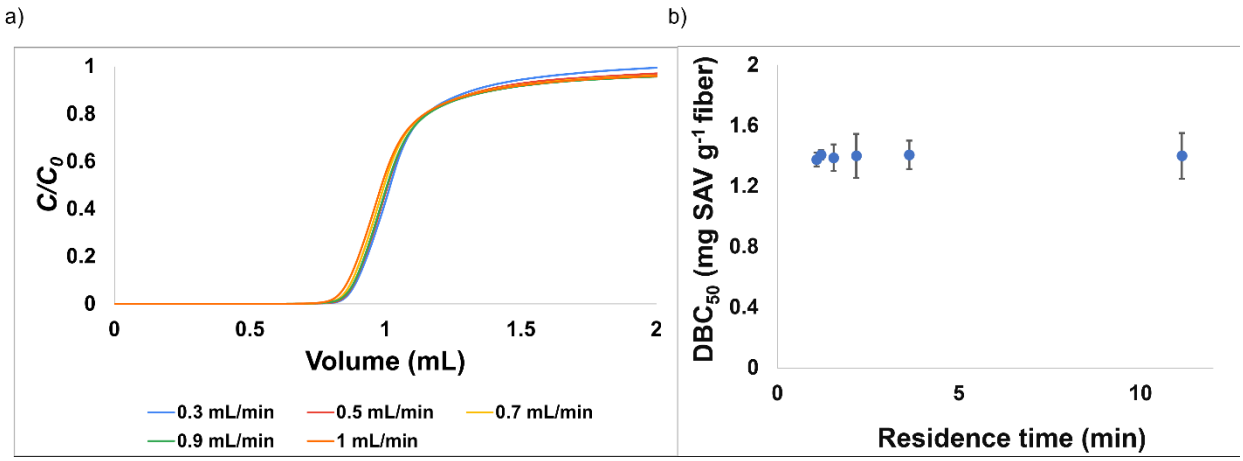

Fig. 2.4 a) Breakthrough curves for 0.5 mg mL^{-1} SAV loading on C-CP fiber columns at different flow rates. b) DBC$_{50}$ plotted as a function of column residence time

of volume flow rates of SAV loading on the C-CP columns. The calculated DBC$_{50}$ values suggest that the mobile phase flow rate has virtually no effect on the SAV adsorption process, yielding dynamic binding capacities ranging from 1.37 to 1.41 mg g^{-1} of fiber, a variability of only 0.87 %RSD across these experiments. The uniformity of the adsorption process is reinforced in Fig. 4b where the DBC$_{50}$ values are plotted as a function of the column residence time for different flow rates. The residence time (a function of the void column volume, flow rate and the column length) can influence the SAV binding to the PP surface. Typically, a longer residence time might suggest greater probabilities for ligand adsorption onto the fiber surface, and indeed greater propensities for multilayering to occur. However, the case is different here for SAV as the DBC$_{50}$ values are found to be virtually identical across the different flow rates. The highest flow rate (1 mL min^{-1})

employed here yields a column residence time of 1.08 min which is sufficient for the column to reach full capacity. Here again, the lower residence times (higher flow rates) show a bit more variability in the data, perhaps suggesting the onset of non-ideal behavior. Since the loading flow rate has minimal effect on SAV loading, a middle range flow rate of 0.5 mL min^{-1} for 3 min was chosen as the SAV loading conditions for further efforts, with an SAV binding capacity of 1.4 mg g^{-1} fiber.

2.3.2 Capture of biotinylated proteins on SAV-modified columns -

The primary focus of this effort lies in the overall effectiveness of the SAV immobilized fiber support phase for the successful capture of biotinylated proteins. The quality of any selective protein capture strategy relies on the ability to have maximum target species capture while minimizing the amount of non-specific binding. The binding of biotin to avidin/streptavidin is a rapid and specific process that is recognized as the strongest noncovalent interaction in nature.[11] Despite its effectiveness, non-specific binding to either the ligand or the support can interfere with the desired binding between biotinylated molecule and streptavidin. Therefore, non-specific binding requires careful consideration and evaluation. There is no practical means to bind-and-elute the affinity-captured proteins due to the strength of the biotin-strepadivin interaction, so that obvious means of assessing binding characteristics (i.e., via the recovery response) is not available. Thus, the process illustrated in Fig. 2 was employed to characterize the fraction of native and biotinylated proteins retained on-column with the former used as a measure of non-specifically bound retention. As will be shown later, the absolute dynamic binding on the column for b-BSA and b-GFP is 131.9 µg and 170.9 µg, respectively. However, in each case, 4 µg of each of the respective proteins was injected onto the SAV-modified

PP fiber column which is below the total binding capacity so that variations in the amount of capture can be observbed across different conditions (i.e. flow rate, buffer concentrations) without evolind aspects of column overload. The amounts of native BSA and GFP that were retained on the SAV-modified columns were compared to the amount of specifically-bound, biotinylated versions of the proteins. The results presented in Fig. 5 demonstrate the capture efficiencies of b-BSA and b-GFP on streptavidin surfaces. It is observed that b-BSA exhibits a capture efficiency of 48.7% (5.4 μg g^{-1} fiber), while b-GFP shows significantly higher capture efficiency of 98.7% (11.02 μg g^{-1} fiber) . From the Avi-tag preparation of the biotinylated proteins it was assumed that the biotinylation rate was one biotin per GFP molecule, whereas the b-BSA most likely has several biotins per BSA molecule. Therefore, differential capture efficiency are not likely based on the biotinylation

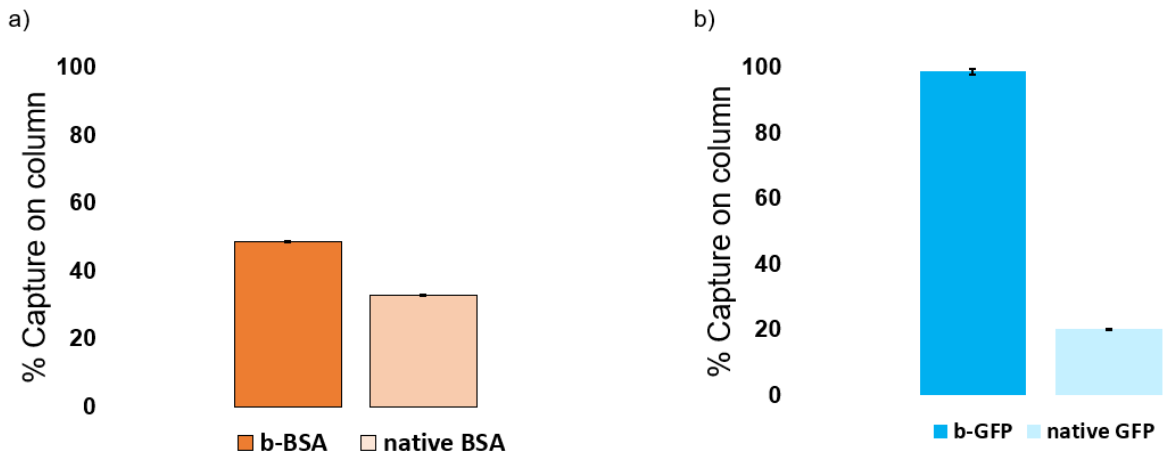

Fig. 2.5 Capture efficiencies calculated from the recovery of a) b-BSA and BSA injections, b) b-GFP and GFP injections

process, but rather the higher capture for b-GFP perhaps reflects the smaller globular structure of the protein (MW = 27 kDa) that might experience less steric hindrance with the SAV binding sites in comparison to the b-BSA (MW = 66.5 kDa).[48, 49] However, the non-specific binding of the native proteins is appreciable with BSA exhibiting a retention

of 32% of the injected protein, whereas the native GFP is retained at a level of 20%. These results demonstrate the preferential ability of the target proteins to bind to the SAV-modified PP fiber surfaces while also pointing to appreciable non-specific retention which must be minimized for high quality purification and pull-down performance.

2.3.3 Effect of flow rate on b-BSA and b-GFP capture –

The optimization process of protein adhesion to SAV-modified fiber surface involves a careful balance between thermodynamics and kinetics. Thermodynamics (i.e., surface affinity) energetically drives the proteins to bind to the surface, while kinetics may impose limitations on mass transfer. As such, a unique balance may exist in that high-affinity interactions can occur on faster time scales than non-selective ones, meaning that solution flow rate/column residence time can be used to potentially minimize non-specific binding in lieu of the targeted capture. In order to elucidate the potential influence of flow rate on selective capture, we present Fig. 6, illustrating the impact of varying flow rates on the capture efficiency of b-BSA and b-GFP. Mobile phase flow rates ranging from 0.25 mL min^{-1} to 1 mL min^{-1} were employed. A four-fold increase in solution flow rate does not yield any significant change in the capture efficiency for both b-BSA and b-GFP. This contrasts with previous protein loading experiments conducted on C-CP fibers where increasing the loading flow rate resulted in reduced protein capture.[24, 35, 40] The disparity in findings can be attributed to the distinct hydrodynamics of the analytical column employed in this study which allows longer residence time in comparison to the microbore column used in prior studies (minutes here versus seconds in the previous studies).[35] Also shown in Fig. 6 are the corresponding retention rates for the native forms of the proteins. In both cases, the biotinylated proteins and native species show little influence

regarding flow rates with the percentage of higher retention of the labeled species remaining constant. While no kinetic differences are seen here for specific vs.

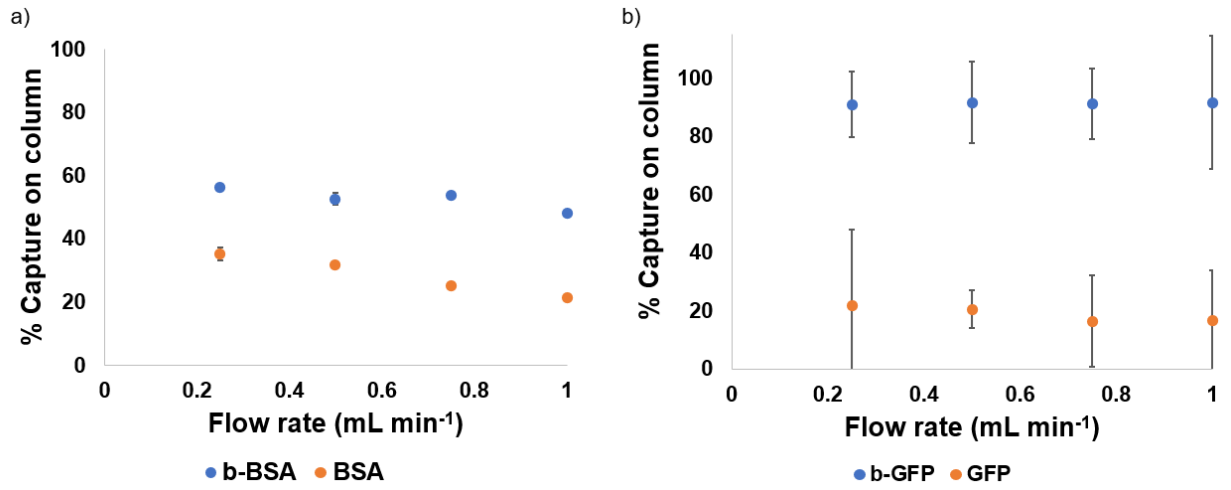

Fig. 2.6 Capture efficiency calculated from the injection recovery at different flow rates of a) b-BSA and BSA, and b) b-GFP and GFP

non-specific binding, experiments discussed in later sections point to definitive kinetic differences when both biotinylated and native species exist in the same solution. Overall, this data holds promise for loading biotinylated proteins with a higher flow rates without any decrease in their binding capacity and yield as seen in protein A-IgG studies.[34] Based on these results, a mobile phase flow rate of 0.5 mL min^{-1} was selected for further investigations.

2.3.4 Loading buffer composition -

In the context of the selective binding performance of immobilized protein surface, loading buffer composition is crucial in generating high-quality binding data and optimizing performance. Various strategies can be employed to address non-specific interactions including adjustment of buffer pH, incorporation of protein blocking additives, elevation of salt concentration, and introduction of non-ionic surfactants. These approaches have

been successfully implemented in diverse experimental methods to control non-specific interactions.[50, 51] Among the options for dealing with non-specific binding caused by hydrophobic interactions, the use of non-ionic surfactants such as Tween-20 is one of the most effective approaches.[52] The addition of small quantities of this mild detergent can effectively interfere with the hydrophobic interactions between the analyte (protein) and the chromatographic surface, thereby mitigating non-specific binding. This strategy holds the potential for reducing undesired interactions and improving the specificity of the binding event. As indicated, Tween-20 functions as a gentle detergent and its influence on the bound SAV on the fiber was not anticipated to result in displacement or degradation. Experiments were conducted to confirm the ligand layer integrity in the presence of Tween-20 prior to the protein capture step, with no appreciable loss in SAV determined. (Further details regarding this experiment can be found in Supplementary Information.)

To investigate the impact of mobile phase composition on capture efficiency and non-specific binding, Tween-20 concentrations ranging from 0.25-to-1% in PBS were employed as the mobile phase. As shown in Fig. 7, the capture efficiency of b-BSA increases with the rise in Tween-20 concentration. To be exact, with a four-fold

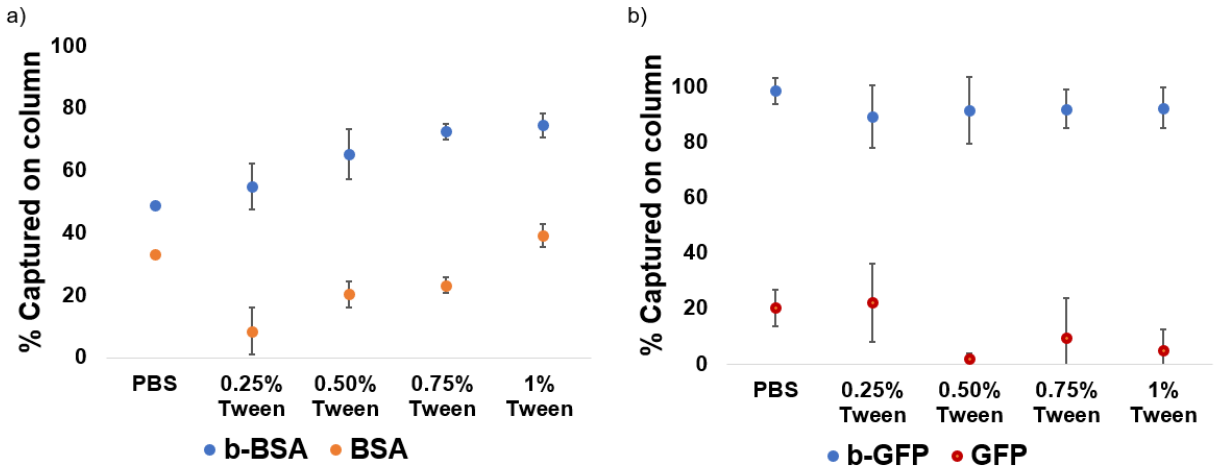

Fig. 2.7 Effect of tween-20 concentration on the capture efficiency of a) b-BSA and BSA and b) b-GFP and GFP. Flow rate : 0.5 mL min^{-1}

increase in concentration (from 0.25% to 1%), the capture efficiency of b-BSA exhibits an increase of ~ 50%. However, it should be noted that the role of the surfactant on the non-specific capture of native BSA is not straightforward. While not explicitly evaluated, there may be some difference in fluorescence efficiency of the BSA at different concentrations of Tween. While the 0.25% Tween results in the lowest amount of retention, the use of 0.5% perhaps represents the best compromise between selective capture and minimized non-specific binding. In contrast, the capture efficiency of b-GFP remains consistent with the increases in Tween-20 concentration. Here, the non-specific GFP capture also does not follow a straightforward trend, although a notable decrease in non-specific capture of GFP is observed at 0.5% and 1% Tween-20 in PBS. These findings indicate the varying effects of Tween-20 concentration on the capture efficiency of b-BSA and b-GFP. While b-BSA shows an overall increase in capture efficiency with increasing Tween-20 concentration, b-GFP exhibits a more stable capture performance. It is to be noted that the selective binding performance on the SAV modified fiber was determined by the

amount of biotinylated protein bound to the column in comparison to the protein loaded at the column by-pass position. Exploring its efficacy relative to a non-SAV loaded column (i.e., unmodified PP fiber) under non-binding conditions could offer valuable insights. Notably, the minimal non-specific binding was observed at the conditions of 0.25% Tween-20 for BSA and 0.50% Tween-20 for GFP, presenting an avenue for assessing selective binding performance. Therefore, biotinylated proteins were injected under these conditions with SAV column modified and unmodified. The determined protein capture efficiency, comparing the SAV-modified column to the bare PP fiber surface, yielded 55.3% (6.17 μg g^{-1} fiber) for b-BSA and 95.2% (10.63 μg g^{-1} fiber) for b-GFP. These findings establish an excellent alignment with the employed methodology. In general, and a specific sample type/matrix would require validation, use of 0.5% Tween-20 in the loading in PBS presents a good compromise in terms of selective capture and minimization of non-specific binding.

2.3.5 Dynamic binding capacity of biotinylated proteins and column-to-column reproducibility -

To understand the dynamics of protein adsorption on the SAV-modified PP fiber surfaces, it is critical to analyze the breakthrough curves of the biotinylated proteins. The breakthrough curves of b-BSA and b-GFP on streptavidin-modified PP fiber columns were examined, and the DBC_{50} of each protein was calculated to quantify the maximum amount of protein that can be loaded onto the column. Figure 8 represents the results of the frontal analysis of the breakthrough curves and reveals differences in the DBC_{50} values between b-BSA and b-GFP. The DBC_{50} for b-BSA was determined to be 358 μg g^{-1} of fiber while that for b-GFP was found to be higher at 464 μg g^{-1} of fiber. In terms of the number of

moles adsorbed on the surface, the amount of b-GFP (1.7×10^{-8} moles g^{-1} fiber) is ~3.2 times more than the b-BSA (5.3×10^{-9} moles g^{-1} fiber). The observed discrepancy in molar DBC_{50} values between the two proteins reflects their capture/loading efficiency on the

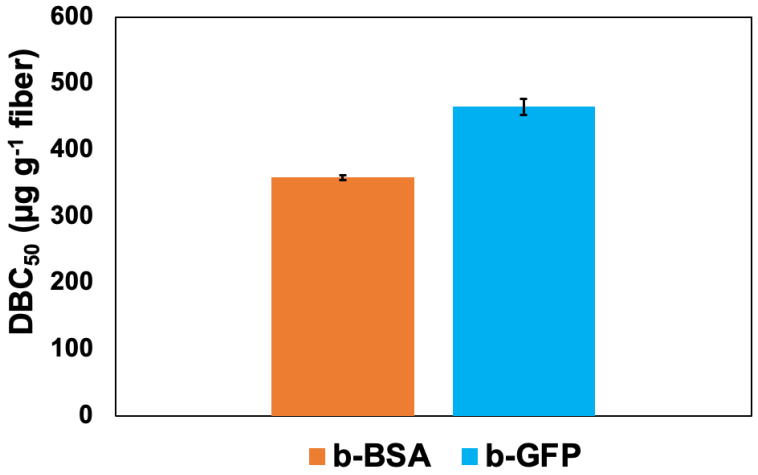

Fig. 2.8 DBC_{50} of biotinylated proteins on SAV-modified fiber columns

column, with the far greater molecular weight/three-dimensional size (r_{Stokes} 3.48 vs 2.82 nm) of the BSA molecule limiting the molar coverage and perhaps overall access to the SAV-modified surface. The molar ratio of the DBC values for the captured b-GFP to the SAV surface ligand is 1:1.4, implying a high level of ligand utilization on the C-CP fiber phase. This high level of utilization provides further evidence for the existence of the SAV as a single-layer system.

To assess column-to-column reproducibility of protein binding, three SAV-modified columns were prepared and b-BSA and b-GFP loaded onto the columns at the concentrations, flow rates, and solvent compositions described above. The percentage relative standard deviation (%RSD) value of the protein binding capacity on column was calculated as a measure of the process reproducibility. As presented in Table 1, The reproducibility of the process is outstanding, with the obtained variability for b-BSA and

b-GFP binding of 2.30 and 5.75 %RSD respectively, reflecting the entirety of the SAV loading process in column formulation as well as the protein capture protocol. This level of performance is outstanding in terms of applications in either protein purification or pull-down applications.

	DBC_{50} of b-BSA on SAV-modified column (μg g^{-1} fiber)	%RSD	DBC_{50} of b-GFP on SAV-modified column (μg g^{-1} fiber)	%RSD
Column-1	368.5	2.30	477.38	5.75
Column-2	354.5		488.55	
Column-3	348.96		427.13	

Table 2.1 DBC_{50} for b-BSA and b-GFP on SAV-modified columns and column-to-column variability.

2.3.6 b-GFP capture efficiency in the presence of background proteins -

The capture efficiency for a targeted protein can be greatly affected by non-specific binding of competitive background proteins to the surface which reduces the number of available binding sites. Effectively, there are kinetic and thermodynamic factors to consider. As fluorescence could be readily utilized (rather than absorbance) as a means of studying such matrix effects on the b-GFP uptake, the extent of such competition was studied for that case. It was determined that the most favorable binding condition, characterized by reduced non-specific GFP binding, was achieved when using a loading solvent containing 0.5% Tween-20 in PBS (Fig. 9). The performance of b-GFP capture in the presence of background proteins was evaluated using a mixture of proteins,

encompassing both “soft” (thyroglobulin and BSA) and “hard” (lysozyme and ribonuclease A) proteins.[53,54] Figure 9 illustrates the b-GFP capture efficiency in presence of the background proteins. Initially, b-GFP was injected onto the streptavidin-modified fiber column, resulting in a capture efficiency of 91.7% and then with the prepared protein mixture and injected onto the column. Notably, b-GFP still exhibits high capture efficiency

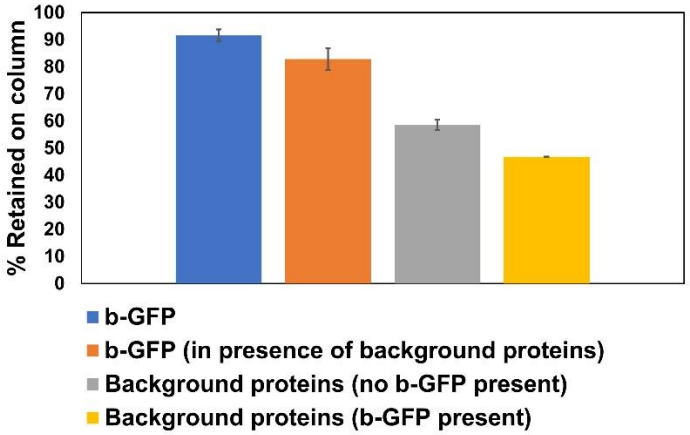

Fig. 2.9 Effect of background protein on b-GFP capture. Loading solvent buffer: 0.5% Tween in PBS. Loading flow rate: 0.5 mL min^{-1}

with a slight decrease and a capture efficiency of 81% observed in the presence of the protein mixture. These results demonstrate that the protein mixture, consisting of both “soft” and “hard” proteins, has only a modest impact on the selective capture efficiency on SAV-modified fiber column. As discussed above, there is a competition between the targeted and non-specifically bound proteins, such that the uptake of the labeled protein would impede the non-specific uptake. To ascertain the affinity of the background proteins to the SAV column alone, the protein mixture was injected onto the column without the presence of b-GFP. Here, the background proteins were retained to a level of 58% when no b-GFP was present. This affinity was moderately reduced to 46% in the presence of b-GFP within the mixture. The occurrence of non-specific capture remains notable even

in the presence of b-GFP. It is important to acknowledge that the background protein mixture encompasses a spectrum of both “soft” and “hard” proteins, prone to binding with hydrophobic surfaces. Moreover, any exposed surface area of the PP substrate (under conditions of admitted under-loading) will contribute to non-specific binding. Therefore, the reduction of background protein interaction requires further optimization. However, it proves well that the rapid capture kinetics eventually preclude the uptake of the native proteins in the targeted capture case, while the b-GFP binding performance is not affected significantly in the presence of background protein mixture.

2.4 Conclusions

In this work, the polypropylene C-CP fiber surface was investigated as a support phase for SAV immobilization and the eventual capture of biotinylated target proteins. SAV-modified fiber columns were prepared with 3 min on-column loading of SAV on to the bare fiber surface. Optimization of the SAV loading characteristics was performed from the frontal analysis. While higher densities could be readily achieved, an SAV density of 1.4 mg g^{-1} fiber was achieved at a nominally load concentration 0.5 mg g^{-1} and 0.5 mL min^{-1} SAV loading rate. The protein capture efficiency of the modified surface was assessed by injecting two biotinylated proteins: b-BSA and b-GFP. To provide for a more selective binding strategy, with reduced non-specific binding, non-ionic surfactant Tween-20 concentrations in PBS were varied as a loading solvent buffer. Studying the effect of flow rate on the loading buffer indicated that the flow rate has minimal effect on either targeted protein capture as well as the non-specific binding. The capture efficiency of b-GFP at optimized loading conditions is not appreciatively affected in the presence of background-interacting protein mixtures. The C-CP platform demonstrates SAV

immobilization with relatively high ligand utilization, while further optimization is required to reduce non-specific background protein interaction.

Future efforts will focus on the more practical aspect of capturing biotinylated antibodies from complex media, including protein L on the SAV-modified fiber surfaces. Implementation of the SAV-modified C-CP columns to a tip format allows for implementation in highly automated sample manipulation platforms and coupling to 96-well processing formats. The binding capacities of b-BSA and b-GFP on SAV-modified PP surface is 358 μg g^{-1} (0.291 mg mL^{-1}) and 464 μg g^{-1} (0.386 mg mL^{-1}) fiber, respectively, achieved in a flow through mode in <3 min. Beyond the throughputs realized, per tips costs of <<$1 are very attractive in comparison to commercial phases. The lack of universal reporting standards to compare protein pull-down binding capacities among the different commercial platforms, numerous variable formats of immobilization, and discrepancies in the measurement methods (static vs dynamic) are notable.[21] For example, commercial phases, operated under equilibrium binding conditions over tens of minutes provide protein capacities of 10x the C-CP fiber tips as applied here. Ultimately, the entire protein capture/elution process, costs, and throughput must be directly compared to the existing commercial processing platforms and materials in order to establish a benchmark for future improvements.

2.5 Acknowledgements

We would like to acknowledge Linda Grimes and Dr. Caleb Schlachter at Integrated Micro-Chromatography Systems (IMCS) for helpful discussions and providing the stock solutions of biotinylated BSA (b-BSA) and biotinylated GFP (b-GFP).

2.6 References

(1) Xie, W.; Wang, H.; Tong, Y. W.; Sankarakumar, N.; Yin, M.; Wu, D.; Duan, X. Specific purification of a single protein from a cell broth mixture using molecularly imprinted membranes for the biopharmaceutical industry. *RSC Adv.* **2019**, *9*, 23425-23434.

(2) Ghosh, R. Ultrahigh-speed, ultrahigh-resolution preparative separation of protein biopharmaceuticals using membrane chromatography. *J. Sep. Sci.* **2022**, *45*, 2024-2033.

(3) Kianfar, E. Protein nanoparticles in drug delivery: animal protein, plant proteins and protein cages, albumin nanoparticles. *J. Nanobiotech.* **2021**, *19*, 159.

(4) Garcia, C. G.; Patkar, S. S.; Wang, B.; Abouomar, R.; Kiick, K. L. Recombinant protein-based injectable materials for biomedical applications. *Adv. Drug Deliv. Revs.* **2018**, 114673.

(5) Moradi-Kalbolandi, S.; Hosseinzade, A.; Salehi, M.; Merikhian, P.; Farahmand, L. Monoclonal antibody-based therapeutics, targeting the epidermal growth factor receptor family: from herceptin to Pan HER. *J. Pharm. Pharmacol.* **2018**, *70*, 841-854.

(6) Bereli, N.; Yavuz, H.; Denizli, A. Protein chromatography by molecular imprinted cryogels. *J. Liq. Chromatogr. Relat. Technol.* **2020**, *43* (15-16), 657-670.

(7) Eifler, N.; Medaglia, G.; Anderka, O.; Laurin, L.; Hermans, P. Development of a novel affinity chromatography resin for platform purification of lambda fabs. *Biotechnol. Prog.* **2014**, *30* (6), 1311-1318.

(8) Arora, S.; Saxena, V.; Ayyar, B. V. Affinity chromatography: A versatile technique for antibody purification. *Methods* **2017**, *116*, 84-94.

(9) de Boer, E.; Rodriguez, P.; Bonte, E.; Krijgsveld, J.; Katsantoni, E.; Heck, A.; Grosveld, F.; Strouboulis, J. Efficient biotinylation and single-step purification of tagged transcription factors in mammalian cells and transgenic mice. *Proc. Nat. Acad. Sci.* **2003**, *100* (13), 7480-7485.

(10) Aissa, A. B.; Herrera-Chacon, A.; Pupin, R.; Sotomayor, M.; Pividori, M. Magnetic molecularly imprinted polymer for the isolation and detection of biotin and biotinylated biomolecules. *Biosens. Bioelectron.* **2017**, *88*, 101-108.

(11) Green, N. M. [5] Avidin and streptavidin. In *Methods Enzymol.* **1990**, *184*, 51-67.

(12) Kim, D. I.; Roux, K. J. Filling the void: proximity-based labeling of proteins in living cells. *Trends Cell. Biol.* **2016**, *26* (11), 804-817.

(13) Wu, K. K. Analysis of protein-DNA binding by streptavidin-agarose pulldown. *Gene Mapping, Discovery, and Expression: Methods and Protocols* **2006**, 281-290.

(14) Luong, J. H.; Male, K. B.; Glennon, J. D. Biotin interference in immunoassays based on biotin-strept (avidin) chemistry: an emerging threat. *Biotechnol. Adv.* **2019**, *37* (5), 634-641.

(15) Wollscheid, B.; Bausch-Fluck, D.; Henderson, C.; O'brien, R.; Bibel, M.; Schiess, R.; Aebersold, R.; Watts, J. D. Mass-spectrometric identification and relative quantification of N-linked cell surface glycoproteins. *Nat. Biotechnol.* **2009**, *27* (4), 378-386.

(16) Frei, A. P.; Moest, H.; Novy, K.; Wollscheid, B. Ligand-based receptor identification on living cells and tissues using TRICEPS. *Nat. Protoc.* **2013**, *8* (7), 1321-1336.

(17) Pfaunmiller, E. L.; Paulemond, M. L.; Dupper, C. M.; Hage, D. S. Affinity monolith chromatography: a review of principles and recent analytical applications. *Anal. Bioanal. Chem.* **2013**, *405*, 2133-2145.

(18) Haukanes, B. I.; Kvam, C. Application of magnetic beads in bioassays. *Bio-Technol.* **1993**, *11*, 60-63.

(19) Filon, M.; Yang, B.; Schehr, J.; Singh, A.; Bigarella, M.; Denu, J.; Lang, J.; Jarrard, D. Abstract B051: Alterations in SIRT2-H3K18Ac identify increased P300 activity in circulating tumor cells from patients with CRPC. *Cancer Research* **2023**, *83* (11_Supplement), B051-B051.

(20) Hussan, R. H.; Dubery, I. A.; Piater, L. A. Identification of MAMP-responsive plasma membrane-associated proteins in Arabidopsis thaliana following challenge with different LPS chemotypes from Xanthomonas campestris. *Pathogens* **2020**, *9* (10), 787.

(21) Berg-Luecke, L.; Gundry, R. L. Assessment of streptavidin bead binding capacity to improve quality of streptavidin-based enrichment studies. *J. Proteome Res.* **2020**, *20* (2), 1153-1164.

(22) Sista, R. S.; Eckhardt, A. E.; Srinivasan, V.; Pollack, M. G.; Palanki, S.; Pamula, V. K. Heterogeneous immunoassays using magnetic beads on a digital microfluidic platform. *Lab Chip* **2088**, *8*, 2188-2196.

(23) Nelson, D. M.; Marcus, R. K. Characterization of capillary-channeled polymer fiber stationary phases for high-performance liquid chromatography protein separations: comparative analysis with a packed-bed column. *Anal. Chem.* **2006**, *78* (24), 8462-8471.

(24) Stanelle, R. D.; Marcus, R. K. Nylon-6 capillary-channeled polymer (C-CP) fibers as a hydrophobic interaction chromatography stationary phase for the separation of proteins. *Anal. Bioanal. Chem.* **2009**, *393*, 273-281.

(25) Wang, L.; Marcus, R. K. Evaluation of protein separations based on hydrophobic interaction chromatography using polyethylene terephthalate capillary-channeled polymer (C-CP) fiber phases. *J. Chromatogr. A* **2019**, *1585*, 161-171.

(26) Bruce, T. F.; Slonecki, T. J.; Wang, L.; Huang, S.; Powell, R. R.; Marcus, R. K. Exosome isolation and purification via hydrophobic interaction chromatography using a polyester, capillary-channeled polymer fiber phase. *Electrophoresis* **2019**, *40* (4), 571-581.

(27) Huang, S.; Bruce, T. F.; Ding, H.; Wei, Y.; Marcus, R. K. Rapid isolation of lentivirus particles from cell culture media via a hydrophobic interaction chromatography method on a polyester, capillary-channeled polymer fiber stationary phase. *Anal. Bioanal. Chem.* **2021**, *413*, 2985-2994.

(28) Fornea, D. S.; Wu, Y.; Marcus, R. K. Capillary-channeled polymer fibers as a stationary phase for desalting of protein solutions for electrospray ionization mass spectrometry analysis. *Anal. Chem.* **2006**, *78* (15), 5617-5621.

(29) Burdette, C. Q.; Marcus, R. K. Solid Phase Extraction of Proteins from Buffer Solutions Employing Capillary Channeled Polymer (C-CP) Fibers as the Stationary Phase. *Analyst* **2013**, *138*, 1098-1106.

(30) Jackson, K. K.; Powell, R. R.; Bruce, T. F.; Marcus, R. K. Solid Phase Extraction of Exosomes from Diverse Matrices via a Polyester Capillary-Channeled Polymer (C-CP) Fiber Stationary Phase in a Spin-Down Tip Format. *Anal. Bioanal. Chem.* **2020**, *412*, 4713-4724.

(31) Jiang, L.; Jin, Y.; Marcus, R. K. Polyethylenimine Modified Poly(ethylene terephthalate) Capillary Channeled-Polymer (C-CP) Fibers for Anion Exchange Chromatography of Proteins. *J. Chromatogr. A* **2015**, *1410*, 200-209.

(32) Jiang, L.; Marcus, R. K. Microwave-assisted, grafting polymerization modification of Nylon 6 capillary-channeled polymer fibers for enhanced weak cation exchange protein separations. *Anal. Chim. Acta* **2017**, *954*, 129-139.

(33) Jiang, L.; Marcus, R. K. Biotin functionalized poly(ethylene terephthalate) capillary-channeled polymer fibers as HPLC stationary phase for affinity chromatography. *Anal. Bioanal. Chem.* **2015**, *407*, 939-951.

(34) Schadock-Hewitt, A. J.; Marcus, R. K. Initial evaluation of protein A modified capillary-channeled polymer fibers for the capture and recovery of immunoglobulin G. *J Sep Sci* **2014**, *37* (5), 495-504.

(35) Trang, H. K.; Schadock-Hewitt, A. J.; Jiang, L.; Marcus, R. K. Evaluation of loading characteristics and IgG binding performance of Staphylococcal protein A on polypropylene capillary-channeled polymer fibers. *J. Chromatogr. B* **2016**, *1015*, 92-104.

(36) Trang, H. K.; Marcus, R. K. Application of protein A-modified capillary-channeled polymer polypropylene fibers to the quantitation of IgG in complex matrices. *J. Pharm. Biomed. Anal.* **2017**, *142*, 49-58.

(37) Marcus, R. K.; Davis, W. C.; Knippel, B. C.; LaMotte, L.; Hill, T. A.; Perahia, D.; Jenkins, J. D. Capillary-channeled polymer fibers as stationary phases in liquid chromatography separations. *J. Chromatogr. A* **2003**, *986* (1), 17-31.

(38) Randunu, K. M.; Marcus, R. K. Initial evaluation of protein throughput and yield characteristics on nylon 6 capillary-channeled polymer (C-CP) fiber stationary phases by frontal analysis. *Biotechnol. Prog.* **2013**, *29* (5), 1222-1229.

(39) Randunu, J. M.; Dimartino, S.; Marcus, R. K. Dynamic Evaluation of Polypropylene Capillary-Channeled Fibers as a Stationary Phase in High Performance Liquid Chromatography. *J. Sep. Sci.* **2012**, *35*, 3270-3280.

(40) Randunu, K. M.; Marcus, R. K. Microbore polypropylene capillary channeled polymer (C-CP) fiber columns for rapid reversed-phase HPLC of proteins. *Anal. Bioanal. Chem.* **2012**, *404*, 721-729.

(41) Raniolo, S.; Vindigni, G.; Ottaviani, A.; Unida, V.; Iacovelli, F.; Manetto, A.; Figini, M.; Stella, L.; Desideri, A.; Biocca, S. Selective targeting and degradation of doxorubicin-loaded folate-functionalized DNA nanocages. *Nanomed. Nanotechnol.* **2018**, *14* (4), 1181-1190.

(42) Ma, M.; Zhuang, F.; Hu, X.; Wang, B.; Wen, X.-Z.; Ji, J.-F.; Xi, J. J. Efficient generation of mice carrying homozygous double-floxp alleles using the Cas9-Avidin/Biotin-donor DNA system. *Cell Res.* **2017**, *27* (4), 578-581.

(43) Zareh, S. K.; Wang, Y. M. Single-molecule imaging of protein adsorption mechanisms to surfaces. *Microsc. Res. Techniq.* **2011**, *74* (7), 682-687.

(44) Gritti, F.; Piatkowski, W.; Guiochon, G. Comparison of the adsorption equilibrium of a few low-molecular mass compounds on a monolithic and a packed column in reversed-phase liquid chromatography. *J. Chromatogr. A* **2002**, *978*, 81-107.

(45) Schadock-Hewitt, A. J.; Marcus, R. K. Loading characteristics and chemical stability of head group-functionalized PEG-lipid ligand tethers on polypropylene capillary-channeled polymer fibers. *J. Sep. Sci.* **2014**, *37*, 3595-3602.

(46) Straut, C. M.; Marcus, R. K. Small molecule adsorption on to polyester capillary-channeled polymer fibers: Frontal analysis of naphthalene and naphthol (naphthalene and naphthol adsorption on capillary-channeled polymer fibers). *J. Sep. Sci.* **2010**, *33* (1), 46-60.

(47) Guichon, G.; Felinger, A.; Shirazi, D. G.; Katti, A. M. Fundamentals of Preparative and Nonlinear Chromatography; *Academic Press*, **2006**.

(48) Demonte, D.; Dundas, C. M.; Park, S. Expression and purification of soluble monomeric streptavidin in Escherichia coli. *Appl. Microbiol. Biot.* **2014**, *98*, 6285-6295.

(49) Pavoor, T. V.; Cho, Y. K.; Shusta, E. V. Development of GFP-based biosensors possessing the binding properties of antibodies. *Proc. Nat. Acad. Sci.* **2009**, *106* (29), 11895-11900.

(50) Désormeaux, A.; Blochet, J.-E.; Pézolet, M.; Marion, D. Amino acid sequence of a non-specific wheat phospholipid transfer protein and its conformation as revealed by infrared and Raman spectroscopy. Role of disulfide bridges and phospholipids in the stabilization of the α-helix structure. *BBA-Protein Struct. M.* **1992**, *1121* (1-2), 137-152.

(51) Situ, C.; Wylie, A. R.; Douglas, A.; Elliott, C. T. Reduction of severe bovine serum associated matrix effects on carboxymethylated dextran coated biosensor surfaces. *Talanta* **2008**, *76* (4), 832-836.

(52) Kenna, J.; Major, G.; Williams, R. Methods for reducing non-specific antibody binding in enzyme-linked immunosorbent assays. *J. Immunol. Methods* **1985**, *85* (2), 409-419.

(53) Norde, W.; Lyklema, J. Interfacial behaviour of proteins, with special reference to immunoglobulins. A physicochemical study. *Adv. Colloid. Interfac.* **2012**, *179*, 5-13.

(54) Benavidez, T. E.; Torrente, D.; Marucho, M.; Garcia, C. D. Adsorption of soft and hard proteins onto OTCEs under the influence of an external electric field. *Langmuir* **2015**, *31* (8), 2455-2462.

CHAPTER THREE

ISOLATION AND QUANTIFICATION OF HUMAN URINARY EXOSOMES USING A TWEEN-20 ELUTION SOLVENT FROM POLYESTER, CAPILLARY-CHANNELED POLYMER FIBER COLUMNS

3.1 Introduction

Extracellular vesicles (EVs) are nanometer-sized, membrane-enclosed vesicles secreted by cells, containing a diverse cargo of bioactive molecules, including proteins, lipids, messenger RNAs, and DNA, all reflecting their cell of origin.[1, 2] More specifically, exosomes, a subset of EVs having sizes ranging from 30 to 200 nm, are secreted by almost all cell types and are found in most body fluids. They serve as messengers relaying cellular information and function in several intricate physiological and pathological processes.[3, 4] Exosomes also carry distinct cell-specific surface biomarkers, allowing their biological origins to be determined. Notably, exosomes are extremely stable and plentiful in biological fluids such as urine, making them ideal for non-invasive sampling, with their cargo and outer-vesicle protein composition providing diverse access as possible biomarkers.[5] Increased secretion of exosomes in numerous pathological states, such as cancer, indicates that exosomes may be useful for diagnostic purposes.[6] Moreover, exosomes actively engage in intercellular communication, effecting the transfer of cargo to target cells and therefore serving as vital disease mediators.[7] This same basic concept of targeted cargo delivery is the basis for the rapidly evolving use of exosomes as vectors for biotherapeutics delivery.[8, 9]

As the field moves towards using EVs as diagnostic biomarkers,[10] drug delivery vehicles,[9] and therapeutic agents in their own right,[11] it is imperative to develop precise and efficient exosome isolation and quantification methods. As a wide variety of exosome

isolation methods are available to affect fundamental biochemistry, clinical, and large-scale processing, it is essential to recognize that no universally applicable method exists. The selection of an isolation approach should be dictated by the subsequent characterization and intended use of the exosomes / EVs. A key consideration of exosome isolation protocol includes yield (microvesicles per unit volume of primary matrix), purity (EVs per mass of residual protein in the isolate), and the preservation of their physical and chemical integrity. Ultracentrifugation (UC), the most widely employed method, presents challenges in terms of cost and time, often requiring lengthy centrifugation procedures ranging from 2 hours to overnight to remove contaminants and large vesicles, still yielding isolates with appreciable protein carryover.[12, 13] Ultrafiltration, a centrifugation-based method, is prone to co-purifying protein aggregates, lacking time efficiency, and may result in the significant loss of exosomes, particularly when isolating from small fluid volumes due to the absorption of vesicles to the membrane.[14] Alternative exosome isolation strategies, such as size exclusion chromatography,[15] immunoaffinity-based capture,[16] and polymeric precipitation,[17] are associated with limitations including low throughput, higher costs and the potential to induce morphological changes.

With the goal of addressing the limitations of other exosome isolation methods, Marcus and coworkers have developed a novel cost-effective approach based on hydrophobic interaction chromatography (HIC) using capillary-channeled polymer (C-CP) fiber stationary phases.[18-23] The fibers, melt-extruded from commodity polymers (nylon 6, polypropylene, and poly(ethylene terephthalate) (PET)), feature a distinctive cross-sectional profile having "legs" that interdigitate when packed to form massive numbers of open (1-4 μm), parallel channels. This configuration, coupled with nonporous surfaces

(on the size scale of proteins and EVs) that inhibits intraphase solute diffusion, allows for high-speed separations (~100 mm s^{-1}) without typical mass transfer limitations of common porous-bead chromatographic phases.[24] These characteristics make the fiber-based columns promising alternatives for exosome isolation in comparison to those traditional methodologies. The method employs both high-performance liquid chromatography (HPLC) column and micropipette spin-down tip formats allowing for solid-phase extraction, with a specific focus on analytical-scale processing. This approach has been successfully employed to extract exosomes from a variety of complex biofluids, including urine, saliva, blood serum, cervical mucus, cell culture media, and plants.[18, 21, 25] Impressively, the technique yields high concentrations of EVs, reaching levels as high as 7×10^{12} EVs mL^{-1} with purities that surpass community standards in all cases and from sub-milliliter initial sample volumes.[23, 26, 27] Furthermore, the method demonstrates remarkable removal efficiency (~95%) of contaminating proteins and lipoproteins from matrices as complex as human serum.[20, 28]

The core aspect driving exosome isolation in the C-CP platform relies on the use of an organic modifier-assisted HIC solvent system. Previously demonstrated organic solvents (e.g. acetonitrile (ACN) and glycerol) have been proven effective in yielding high concentrations of pure EVs from a variety of biofluids and cell culture media.[23, 26] However, both solvents present unique challenges that limit the comprehensive characterization and utility of the isolated EVs. The utilization of high concentrations of ACN (50%) can potentially impact the long-term stability of EVs, though the ability to remove excess ACN by ambient evaporation yields EVs in a virtually pristine PBS matrix for characterization by LC-MS, for example. Glycerol, on the other hand, possesses

cryopreservative properties that support long-term storage of EVs, yet it may interfere with post-isolation characterization, particularly by blocking access to surface marker proteins that are crucial for immune and flow cytometry-based assays.[29] In this case, ultrafiltration is effective for solvent removal, but involves another processing step. In pursuit of an improved HIC-assisted solvent for long-term EV preservation and perhaps greater overall versatility, an alternative approach employing Tween-20, a non-ionic detergent, has been previously explored by this group.[27] That effort demonstrated the potential to isolate high-purity EVs from HEK cells while remaining compatible with subsequent immuno-characterization methods. However, as reported in numerous studies, the use of high-concentrations of detergent may disrupt protein-protein and lipid-lipid interactions in EV membranes, potentially compromising the structural integrity.[30-32] Moreover, elevated concentrations of Tween-20 may not be suitable for certain applications, such as mass spectrometry (MS) proteomic workflows.[33] Therefore, a more detailed evaluation of Tween-20 as an elution solvent was undertaken towards achieving high throughput isolations of high-purity exosomes while preserving their structural integrity.

This effort presents a low-cost, efficient, and gentle HPLC-based isolation protocol of exosomes from human urine utilizing a Tween-20 based HIC methodology on PET C-CP fiber columns. Human urine, a target sample biomatrix in various assays, is readily available and does not require prior concentration or centrifugation steps before injection onto the fiber column. Filtration with a 0.2 µm membrane effectively removes larger contaminants, such as cells, preparing the sample for injection. A step gradient, first to remove matrix proteins and then elution of the exosomes by Tween-20, was employed in

the HIC separation to affect recovery and purification. Exosome quantification relied on in-line optical absorbance detection and the generation of response curves prepared from exosome standards. The integration of standard HPLC absorbance and multi-angle light scattering (MALS) chromatograms enables quantification and size determination; offering an automated, high-throughput approach for purification and characterization. In contrast, most commonly used manual processing methods, such as centrifugation, require off-line characterization on completely separate platforms, potentially introducing operator-dependent variability and potentially impacting the purity of the collected fractions.[34] Verification of morphological integrity of the vesicles was conducted by transmission electron microscopy (TEM) imaging. The micro-BCA protein assay was performed to evaluate isolate purity. The Tween-20 elution flow rate was optimized to achieve high-throughput, high-purity separations. Finally, the method's reproducibility was assessed, incorporating an inter-column washing step to enhance EV purification processing. This methodology holds promise for advancing EV research, offering a reliable and reproducible approach to urine-derived exosome isolation.

3.2 Materials and Methods

3.2.1 Sample preparation -

Ultrapure grade ammonium sulfate ($(NH_4)_2SO_4$) was purchased from thermo scientific (MA, USA). Tween-20 was obtained from Anatrace (OH, USA). HPLC-grade acetonitrile was purchased from VWR Chemicals (Radnor, PA). Deionized (DI) water was obtained from Elga PURELAB flex water purification system (18.2 MΩ-cm) (Veolia Water Technologies, High Wycombe, England). Gibco phosphate buffered saline (PBS) solution 10X pH 7.4 (ThermoScientific, MA, USA) was diluted in DI water to prepare a 1X solution

which served as the stock PBS for further mobile phase solvent preparation. Lyophilized exosome standards derived from human urine of healthy donors were purchased from HansaBioMed Life Sciences (Tallinn, Estonia). These standards have a nominal as-constituted concentration of 1.4×10^{12} particles mL^{-1}. To prepare the exosome standards for further characterization and quantification studies, the lyophilized exosomes were reconstituted using 100 µL of DI-H_2O, following the manufacturer's instructions. It is essential to note that the exosome stock used in this study was not designated as certified reference material, nor is an assay provided as to the absence of residual proteins (i.e., purity values) provided by the supplier. Fresh morning urine was collected from a healthy, consenting donor. The urine sample was filtered using 0.2 µm PES (polyethersulfone) membrane syringe filters, without any additional manipulations, to obtain the sample required for this study.

3.2.2 Instrumentation –

Chromatographic analysis was conducted using the Dionex Ultimate 3000 HPLC system, consisting of the LPG-3400SD quaternary pump and MWD-3000 UV-Vis absorbance detector from Thermo Fisher Scientific (Sunnyvale, CA, USA). The Chromeleon 7 software system was employed to control the HPLC system. A UV detection wavelength of 216 nm was used with the post-column UV-Vis detector during the analysis. A 1 mL HENKE-JECT Tuberculin syringe (Germany) and 100 µL injection loop were used for sample injection.

In-line with the HPLC flow, following the absorbance detector, size determination of isolated exosomes was carried out via multi-angle light scattering (MALS) using a DAWN (Wyatt Technology, Goleta, CA) detection system controlled by ASTRA software.

In a very recent communication,[35] Wysor and Marcus have provided a very detailed description of this particular coupling, factors affecting exosome sizing and number density determinations, and the excellent quantitative agreement between absorbance detection and MALS-determined quantification. Particle eluates from the HPLC HIC elution passed through the MALS detector to determine the RMS radii, with the radii multiplied by 2 to get the approximate diameter of the eluted vesicles. The refractive index utilized for exosome particle sizing and the eluate were set at 1.51 and 1.336, respectively.[36]

3.2.3 Construction of C-CP fiber columns -

The assembly of tri-lobal, polyester (PET) C-CP fiber columns was accomplished using melt-extruded fibers obtained from Universal Fibers (Bristol, VA), and has been described previously.[37] The PET C-CP fiber microbore column format was prepared by pulling 8 rotations of fibers (equating 448 single fibers) through a 30 cm long polyether-ether-ketone (PEEK) tube having an inner diameter of 0.76 mm (IDEX Health & Science LLC, Oak Harbor, WA, USA). This number of fibers is used to achieve an interstitial fraction of ~0.6.[38] Columns with such dimensions can accommodate dynamic loads of ~5 × 10^{12} exosomes,[23] achievable within less than 10 min. After packing, the fiber column was flushed with DI-H_2O, ACN, and then DI-H_2O at a flow rate of 0.5 mL min^{-1} until a stable baseline was achieved with the UV-Vis detection at 216 nm. Once the columns were cleaned, they were stored at ambient conditions for further use.

3.2.4 Exosome isolation and quantification methods -

The standard HIC elution strategy for the isolation of exosomes on PET C-CP fiber columns is very well established, to date using acetonitrile and glycerol as the organic-

modifier elution solvents.[18, 23] The basic elements of the HIC method include sample injection (20 – 100 μL) into the loading solvent of 2M $(NH_4)_2SO_4$, wherein high polarity and ionic species pass through the column and proteins and exosomes are retained on-fiber. This loading step is performed for 5 min. though could be reduced in time if desired. Following column loading, a step gradient is affected, where the salt content is reduced to 1 M $(NH_4)_2SO_4$ with the solvent also containing 20 – 30% of the organic modifier in 1X PBS for a period of 3 – 4 mins. This solvent system is sufficiently polar to remove free (matrix) proteins from the fiber surface, leaving the exosomes immobilized. The choice of the modifier corresponds to the ultimate exosome elution solvent, glycerol or ACN. The most readily implemented exosome elution sequence involves a step gradient where the salt content is reduced to zero, and the organic modifier solution concentration is increased to 40 – 50% in PBS for a period of 3-5 mins. Following the exosome elution, a 90% ACN solvent (in PBS) is applied for 5 min for column washing/regeneration between subsequent analyses The isolation and column cleaning process employed a mobile phase volume flow rate of 0.5 mL min^{-1}.

Key in the development of these step gradient methods has been the use of standard (linear) gradient elution protocols to establish the necessary solvent strengths for the sequential removal of the background proteins and the target EVs. In the evaluation of Tween-20 as an elution solvent, a 20% ACN in PBS protein elution step is employed in all cases prior to the ultimate exosome elution gradient. The ACN organic modifier is chosen here as it presents few potential problems with regards to solvent mixing than glycerol. Following assessment of gradient elution characteristics, step gradients were then evaluated and used as the default process.

Very early studies of the HIC isolation strategy demonstrated the efficacy of absorbance detection and quantification through application of simple Beer's Law based on serial dilutions of EV standards.[18, 19, 27, 39] Eluting species were monitored at 216 nm for UV-Vis absorbance (actually microvesicle scattering). The gradient baseline absorbance was obtained from a chromatogram taken while injecting a blank PBS injection and subtracted from the subsequent gradient exosome isolation chromatograms. The integrated area of the exosome elution peak calculated from Chromeleon 7 software represents the quantity of eluted species. To quantify the Tween-20 eluted exosomes, similar isolation procedures were applied to the human urinary exosome standards of five different concentrations (4.3×10^{10} - 7×10^{11} exosomes mL^{-1}) to generate a response curve. A 100 µL injection volume was used for each sampling, and the response curve was constructed from triplicate injections of each. Based on the detector response of elution bands, analytical fractions were collected following elution from the MALS cell and stored for further characterization (e.g., TEM, protein purity assay).

3.2.5 Transmission Electron Microscopy (TEM) -

The physical identification and structural integrity of isolated EVs was characterized using TEM imaging using a Hitachi HR7830. To initiate the sample preparation, 7 µl of each recovery from the human urine sample isolation was carefully deposited onto EM-grade copper/formvar grids and allowed to incubate at room temperature for 20 min. Following incubation, the excess sample liquid was removed from the grids by wicking using a paper towel. The immobilized vesicles were immediately subjected to fixation using a 2% paraformaldehyde solution at room temperature for 5

min. Any surplus paraformaldehyde was removed from the grids using a paper towel. The grids were then gently washed with water for 5 min, ensuring the elimination of any residual reagents. Staining of the EVs immobilized on the grids was achieved by applying a filtered 1% uranyl acetate solution at room temperature for a brief period of 1 min. Following the staining process, excess staining solution was thoroughly removed, and the prepared grids were once again washed with water to guarantee the removal of any excess staining reagent. Lastly, the prepared TEM grids were allowed to dry overnight within a sterile cell culture dish. To ensure the absence of moisture during the drying process, a desiccator was employed, with the procedure carried out at room temperature. This detailed protocol provides a standardized and reproducible method for the TEM imaging of EVs, ensuring the preservation of their structural integrity and enabling accurate morphological analysis.

3.2.6 Exosome isolate purity assessment via micro BCA protein assay -

A standard micro BCA assay was employed to determine the residual protein concentration in the Tween-20 isolated exosome fractions. To be clear, while a value of zero residual protein would be ideal, the micro BCA determination will also register positively for the proteinaceous species incorporated in the exosome vesicular structure. The suggested practical target for describing exosome isolates as being of *high purity* is a value of 3×10^{10} EV μg^{-1} protein.[40, 41] In the micro BCA assay, a 100-µL aliquot of the sample was combined with 50 µL of PBS and 150 µL of the assay working reagent. Subsequently, the 96-well plates were covered and incubated at 37 °C for 2 hours. The absorbance at 562 nm was measured utilizing a Synergy H1 Hybrid plate reader. For accurate protein quantification in unknown samples, a standard curve was generated

using bovine serum albumin (BSA) standard solutions. The average absorbance reading of the blank (PBS) was subtracted from the standards and the EV samples. All measurements were conducted in triplicate, ensuring the reliability of the results.

3.3 Results and Discussion

3.3.1 Chromatographic isolation of exosomes -

Our prior investigation demonstrated the successful isolation of exosomes from the supernatant of an HEK-293 cell culture utilizing 1% Tween-20 as the elution solvent in a PET C-CP fiber spin-down tip format.[27] The physical characteristics, encompassing shape and size distribution of the isolated exosomes, were confirmed using TEM and MALS, respectively. The method was particularly efficient as 10^{12} EVs could be obtained from only 100 μL aliquots of milieu, with the exosome purity of the isolates exceeding the target values by 1 -2 orders of magnitude in all cases. Despite this success, It is crucial to consider the fact that micelle-forming detergents can induce membrane solubilization.[42, 43] Ionic detergents at much lower concentrations (0.01% SDS) can lead to membrane disruption, impacting the exosomes' physical morphology and bioactivity.[30] While non-ionic detergents, such as Tween-20, are deemed milder in comparison to ionic detergents like SDS, higher concentrations may disrupt lipid-lipid and lipid-protein interactions, posing a risk to the phospholipid bilayer membrane of the isolated exosomes.[32, 44] Therefore, a more thorough evaluation is necessary to utilize minimal concentrations of the detergent to affect maximum EV recovery from the biofluid samples while maintaining the morphology and physical integrity of the isolated vesicles.

In this study, the optimization of Tween-20 as an elution solvent for exosomes isolated from human urine is carried out using the PET C-CP fiber column format on an

HPLC platform. This approach allows use of a conventional linear gradient for a controlled and gradual change in solvent composition following the initial release of the residual proteins using the 20% ACN in PBS step. In this case, a linear gradient of 0 – 0.5%

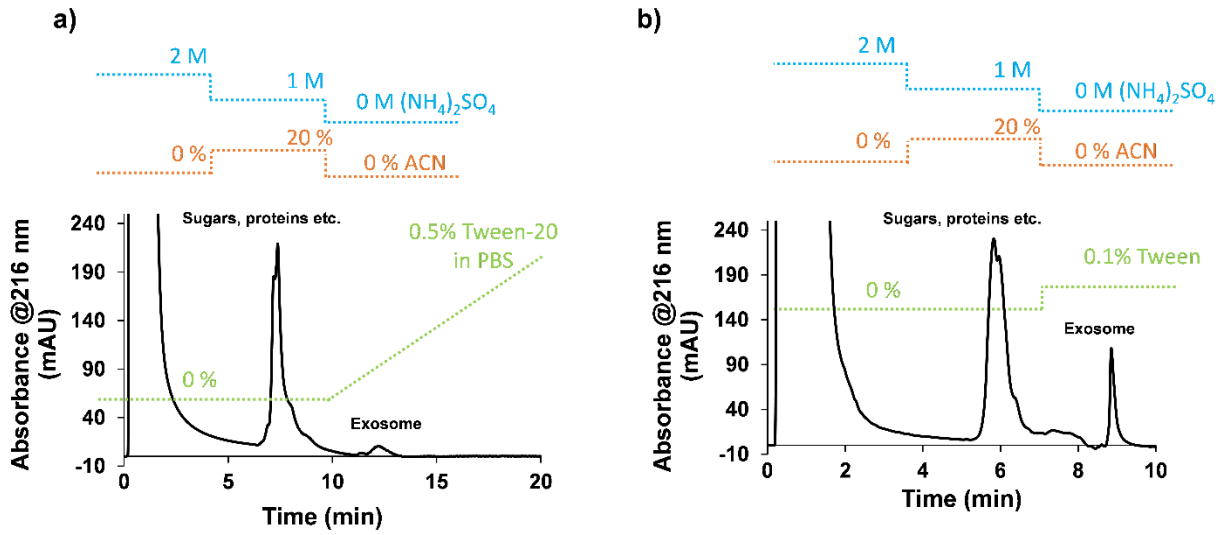

Fig. 3.1 HIC chromatograms of urinary exosome isolation using PET C-CP fibers. a) 10 min gradient from 0 to 0.5% (v/v) Tween-20 in PBS b) step gradient of 0.1% (v/v) Tween-20 (3 min). Protein elution step (1 M $(NH4)_2SO_4$ and 20% ACN) were performed in each case before the isolation of exosomes. 100 µL urine were injected with the flow rate applied 0.5 mL min^{-1}.

Tween-20 was applied for the separation as this was anticipated based on the previous spin-down tip experiments and in consideration of potential vesicle disruption at higher Tween concentrations. A representative chromatographic profile of the gradient elution is presented in Fig. 1a. The large absorbance transient occurring in the 0 – 2 min time frame reflects the injection of the pre-filtered (with a 0.2 µm PES filter) urine sample. Small organic molecules and ionic species are expected to elute in this injection/loading step.[18] As depicted, a step gradient dropping the ammonium sulphate concentration to 1 M, while adding the 20% acetonitrile in PBS is initiated at t = 5 min. The significant peak between

~6 and 9 minutes corresponds to the elution of proteinaceous materials from the fiber column, resulting in a fiber surface composed solely of the adsorbed exosomes. Finally, at t = 10 min, the salt and organic modifier concentration are dropped to “0”, and the linear Tween-20 solvent gradient (0 to 0.5% v/v in PBS) is initiated from t = 10 to 20 min to elute the highly hydrophobic exosomes from the fiber column surfaces. The anticipated elution band between t = ~11and 13 min corresponds to Tween-20 concentrations ranging from 0.08 to 0.16% in PBS. Different from the protein elution band, which has an abrupt onset due to the step nature of the solvent change, the exosomes evolve over a range of solvent strengths which reflects a range of surface interaction strengths; perhaps due to the heterogeneity of exosome sizes and/or surface protein composition.

Based on the elution solvent composition from the linear gradient in Fig. 1a, a step gradient was investigated to shorten the elution time and simplify the elution procedures, as presented graphically in Fig. 1b. In this case, the step gradient times were shortened to minimize processing time and solvent consumption. As in all HIC-based EV separations, salts and ionic small molecules are manifested in the unretained injection peak (~0 – 2 min), while proteins and other non-polar molecules are eluted with the initial gradient step (1 M ammonium sulfate: 20% ACN) initiated at t = 4 min. While the previous spin-down tip method employed 1% Tween-20, clearly that concentration is not required based on the linear gradient results. Indeed, it is reasonable to use as low of a value as practical, to alleviate potential problems. Therefore, exosomes were eluted employing a 0.1% v/v Tween-20 gradient step at t = 7 min, appearing in the chromatogram as a sharp band from ~8.5 – 9.5 min. The application of a total 10-minute gradient, with a focused 3-minute step for exosome elution, demonstrates superior efficiency in comparison to the

linear gradient (Fig. 1a), resulting in shortened processing time, sharper elution bands, improved resolution between the protein and EV eluates, and higher exosome yields. Specifically, the integrated absorbance for exosome elution in the linear gradient was 9.1 mAU*min, while the value for the step gradient was 18.7 mAU*min, a two-fold improvement in recovery. Consequently, the 0.1% Tween-20 step gradient was adopted to advance the development of a Tween-20-based HIC exosome isolation strategy.

3.3.2 Characterization of isolated exosomes -

After assessing basic chromatographic conditions which appear to affect the elution of exosomes, the next question becomes whether or not the particles retain their vesicular structure and some assessment as to the obtained particle size distribution. Transmission electron microscopy (TEM) plays a critical role in the characterization of the isolated exosomes by providing high-resolution images of morphological attributes, allowing inferences of exosome health and likely retention of important cargo.[45, 46] Figure 2a presents a representative micrograph of an exosome collected post-column following elution with 0.1% Tween-20 solvent. The TEM micrograph showcases one of many vesicles with sizes below 200 nm, consistent with the typical range of exosomes (50 – 200 nm). The membrane structure suggests that the method does not compromise the structural integrity of exosomes and that the captured and eluted exosomes are preserved intact. Indeed, ELISA assays for the CD9 and CD81 tetraspanin proteins in the previous spin-down processing with 1% Tween-20 showed that those proteins were retained in the vesicle membranes.[27] It must be reiterated, though, that full verification of vesicle integrity requires some assessment of the cargo (e.g., miRNA) loading; those studies are planned for the near future.

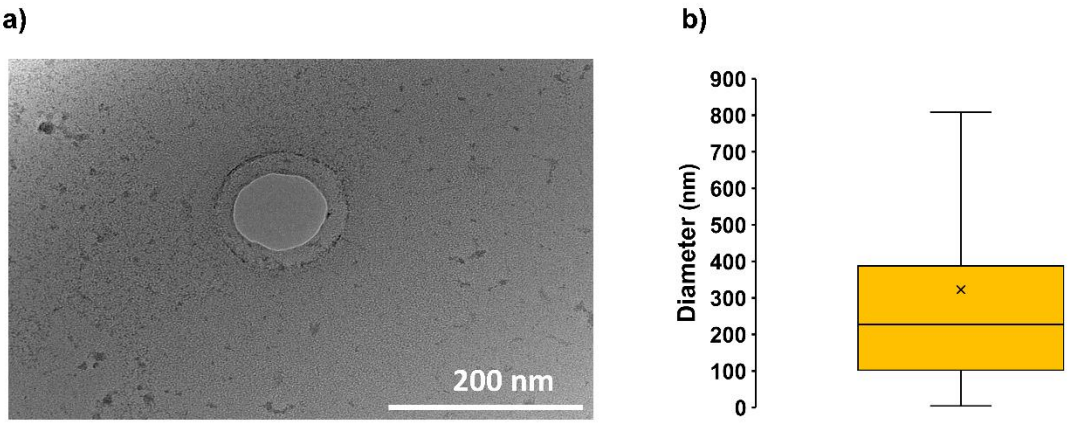

Fig. 3.2 a) Transmission Electron Microscopy (TEM) image of exosome eluted from 0.1% (v/v) Tween-20, b) Post column size determination of the isolated EVs using multi-angle light scattering (MALS) detector.

While TEM provides crucial morphological information, its ability to verify exosome sizing is limited by simple counting statistics. To address this, size verification of isolated fractions was performed using the multi-angle light scattering (MALS) detector, which inherently offers particle/vesicle sizing and number density. A more commonly used method, nano particle tracking analysis (NTA) is susceptive to providing operator dependent results with inconsistencies in precision and accuracy.[36] MALS on the other hand can provide high levels of precision and has been employed in many studies of EV size determinations.[27, 47, 48] Moreover, the integrated approach of combining absorbance and MALS detectors in a standard HPLC instrumentation allows for a comprehensive one-injection determination of the concentration and sizes of eluted exosomes.[35] As illustrated in Fig. 2b, MALS-determined size distributions of urine-derived EVs show that 50% of the population falls in the range of ~100 and 380 nm in diameter. This aligns well with the previously determined size distribution of C-CP tip isolated EVs using Tween-20

from cell culture media, where the average diameter of EVs found to be 249 nm across the cell culture incubation time period.[27] However, it is to be noted that the average size of urinary EVs from Tween-20 isolation and MALS determination are higher than the sizes determined with NTA and organic solvent (ACN)-based isolation in previous studies of this group.[39] There are questions as to the absolute values produced for the Tween isolation as one variable in the MALS calculation has to do with the refractive index of the "particle" which here also includes a likely layer of detergent coverage. That finite layer itself may effect scattering responses. The influence of elution solvent on apparent MALS exosome particle sizes will be a topic of future study.

3.3.3 Quantification of the isolated exosomes -

Prior investigations have established a direct correlation between the concentration of exosomes in solution and the observed amount of light scattering, as manifest in a standard absorbance measurement.[18, 19, 39] This relationship is quantitatively expressed through Beer's law, wherein the quantity of exosomes is proportional to the absorbance peak area. It is to be noted that exosomes are nanometer-sized vesicles which are expected to more efficiently scatter than to absorb 216 nm photons. To obtain a quantitative relationship between exosome concentration and the measured integrated absorbance peak area, six different concentrations of commercial human urine derived exosome standards were applied to generate a standard response curve. Different concentrations of commercial exosome standards (in a range of 4.3×10^{10} - 7×10^{11} exosomes mL^{-1}) were obtained through serial dilution of the primary stock solution, with 100 µL injection volumes loaded onto the column and eluted using the step gradient elution program with 0.1% Tween-20 described in previous section. The data with

regression statistics are presented in Fig. 3, in terms of the injected exosome concentrations and the integrated absorbance values. The agreement aligns with linearity

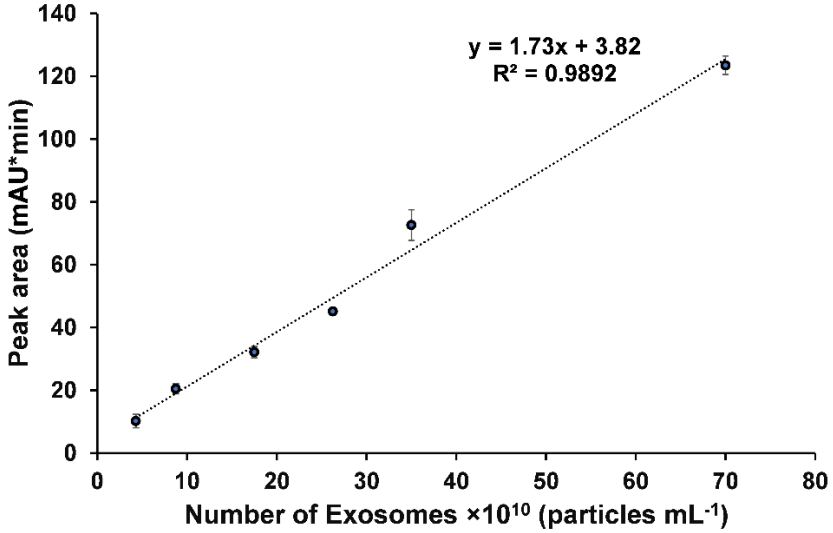

Fig. 3.3 Response calibration curve of the human urine derived exosome standard prepared at different concentrations with 100 µL injection volume, plotted as a function of the number of exosomes injected on column. Triplicate injections were performed for each sample volume.

(R^2 = 0.9892) with a linear response function of y = 2.73x + 3.82, with the range of triplicate values falling within the plotted symbols. Subsequently, a 100 µL human urine sample was injected onto the column and eluted using the same gradient program protocol to determine the concentration of exosomes in the sample. Using the HIC protocol, the urine injection yields an average integrated absorbance of 22.50 ± 0.02 mAU * min for triplicate measurements, representing an exosome recovery concentration of 1.07×10^{11} exosomes mL^{-1}.

3.3.4 Purity assessment of recovered exosomes via micro BCA assay –

A major challenge in all forms of exosome isolation, regardless of the end application, is achieving high purity exosome isolates; i.e., minimizing protein carryover [40, 49]. Previous efforts in this laboratory have shown excellent performance in the case of spin-down tip isolations, regardless of the elution solvent.[21, 25, 27] Indeed, direct comparison to more established methods proves the efficacy of the approach.[26] What has not been established is the purity levels obtainable via the HPLC column methodology and so the purity in terms of protein content of the recovered EV fractions from the human urine samples was determined. The micro BCA protein assay employs a detergent-compatible bicinchoninic acid formulation for the colorimetric detection and quantitation of total protein content.[41]

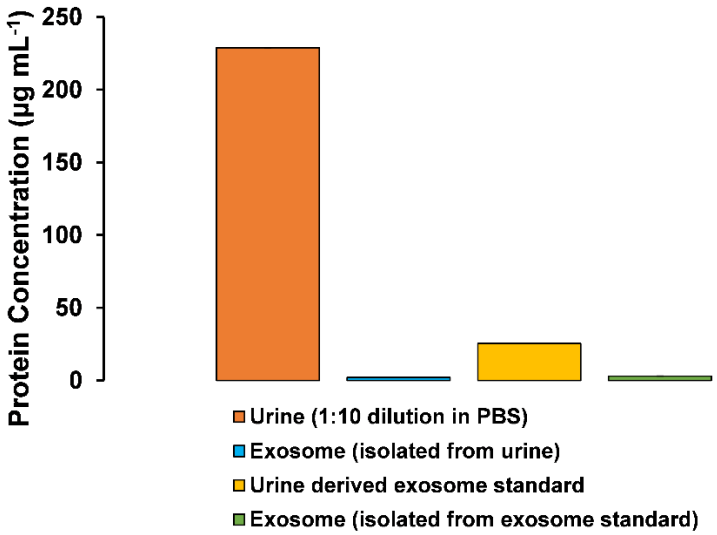

Fig. 3.4 Micro BCA assay-determined protein concentrations in the raw urine sample, EV fraction eluted from the raw urine, the commercial exosome standard, and the EV fraction eluted from the standard, respectively.

Figure 4 represents the micro BCA assay-determined protein concentrations in the raw urine sample, the eluted EV fraction from the raw urine, the reconstituted commercial

exosome standard, and the eluted EV fraction from the standard, respectively. Not surprisingly, the raw human urine (undiluted) sample yielded a concentration value that was beyond the extent of the linear response of the assay; therefore, a dilution of the sample was required (1 : 10 in 1X PBS). Clearly seen, the protein content in the diluted raw urine sample is reduced a significant amount in the eluted EV fraction from 228 μg mL^{-1} to 2.1 μg mL^{-1}, with the lower value equating to the limit of detection (LOD) for the micro BCA assay (LOD = 2 μg mL^{-1}). The extent of the residual protein removal was found to be the same in the case of commercial exosome standard, where the isolation reduces the protein concentration from 25 μg mL^{-1} to 3 μg mL^{-1}. (It is to be noted that a high level of precision was observed for the protein assay, with the variability in each triplicate measurement < 3% RSD.) The determined protein concentrations in the exosome eluates occurring in the vicinity of the LOD underscores both the efficacy of the C-CP fiber processing method and limitations in accurately quantifying the obtained EV purities. That said, the change in total protein content from the diluted raw sample to the eluted fraction corresponds to a >99% reduction in background proteins. As mentioned earlier, the commercial exosome standard is not a certified reference material and its starting material purity value is not provided by the manufacturer.

In assessing the efficacy of any EV isolation method, the crucial metric of interest is the ratio of number of recovered exosomes per unit volume to the protein content within the same volume. In the case of the 0.1 % Tween-20 step gradient HIC method, the purity value obtained for the introduction of raw human urine was ~5×10^{10} EVs per μg of total protein recovered. As noted above, based on limitations to the micro BCA methodology, it is reasonable to say that the obtained purity is actually greater than that value. It is

important to note that the purity value obtained from Tween-20 based C-CP column isolation is within a factor-of-2 of that obtained from C-CP tip isolation employing ACN and glycerol solvents (~1 x 10^{11} EVs μg^{-1} protein) [26], with the differences lying in either the actual urine starting materials or the fact that the column method involves >10x greater elution volumes (dilution) than the tip processing. Regardless, the obtained values exceed the recognized "high purity" standard (> 3×10^{10} EVs per µg of protein).[26,41]

3.3.5 Effect of the mobile phase flow rate -

Consistent throughout the previous applications of C-CP fiber stationary phases to the separation of protein molecules is the fact that higher mobile phase linear velocities provide higher throughput while also delivering higher resolving powers.[50-52] This phenomena is related to the highly efficient solute mass transport through the open parallel channels, formed by the non-porous polymer fibers.[24] To that end, separations at linear velocities up to ~100 mm sec^{-1} have been applied. To the same end, dynamic binding capacities are not sacrificed at high linear velocities.[52] Therefore, it is reasonable to question the efficacy of using high flow rates in the processing of exosomes. In three previous studies, while not as pronounced as the benefits in protein separations, it is consistently true that while lower loading velocities tend to improve the EV binding capacities, higher flow rates yield greater exosome process throughput and recoveries from the fiber columns.[53-55]

The primary assessment of the impact of flow rates on the isolation of urinary exosomes in the 0.1% Tween-20 HIC program, variations of the flow rates (0.3, 0.5, 0.7, and 0.9 mL min^{-1}) in the exosome elution step were performed, as illustrated in Fig. 5 and quantified in Table 1. These flow rates equate to linear velocities of ~24 - 72 mm sec^{-1}.

In this case, the loading flow rate was held constant at 0.5 mL min^{-1}, with 100-µL human urine sample volumes loaded . Qualitatively, the figure reveals that higher flow rates lead to earlier elution times, indicative of the swifter elution process after release, with the concurrent reduction in absorbance responses reflecting the increased dilution (per unit time) in the solution phase within the absorbance cell. This finding is consistent with prior investigations utilizing the HIC isolation method for proteins and EVs on C-CP fiber

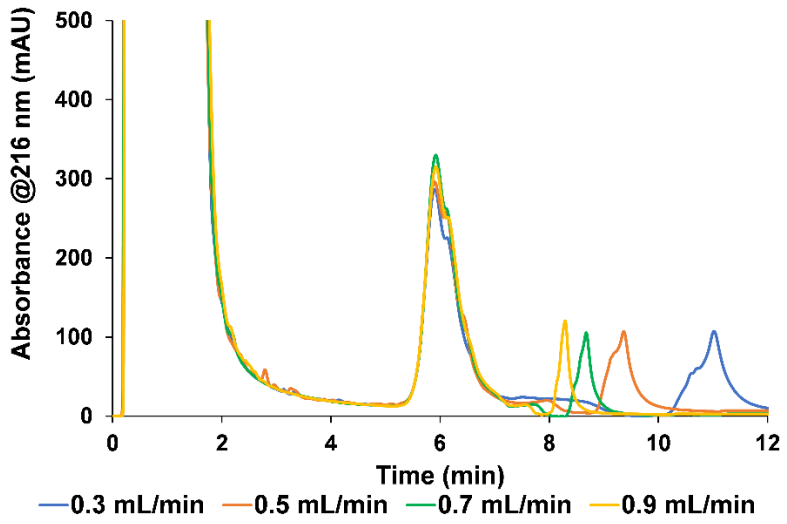

Fig. 3.5 Isolation/recovery of exosomes from human urine as a function of elution flow rate. Flow rate varied at 0.3, 0.5, 0.7, and 0.9 mL min^{-1}, respectively. 100 µL urine was injected each case.

Volume flow rate (mL min^{-1})	Retention time (min)	Peak area (mAU*min)	Peak width
0.3	11.1 ± 0.05	34.03 ± 1.04	0.67 ± 0.05
0.5	9.4 ± 0.01	23.91 ± 1.62	0.63 ± 0.08
0.7	8.6 ± 0.04	16.4 ± 0.52	0.43 ± 0.002
0.9	8.2 ± 0.05	13.3 ± 0.65	0.29 ± 0.002

Table 3.1 Exosome elution peak characteristics from human urine isolation at different elution flow rates. Averages from triplicate measurements with standard deviation values are presented. 100 µL urine was loaded at a flow rate of 0.5 mL min^{-1} for each injection.

phases.[38, 39] The observed trends in elution characteristics can be ascribed to a decrease in longitudinal diffusion (van Deemter B-term) coupled with the absence of solution-solid mass transfer limitations (van Deemter C-term). The decline in absorbance at higher flow rates should be directly proportional to the corresponding dilution factors linked to the increasing flow rates, with the actual values (35.5 to 13.2 mAU * min) suggesting that the recoveries at the higher flow rates are ~35% higher than at the lowest flow rate. These outcomes provide valuable insights into the optimization of flow rates for effective urinary exosome isolation and potential improvements in overall process throughput.

3.3.6 Reproducibility of chromatographic cycles -

Ensuring the consistent recyclability of columns following elution and washing procedures is a critical factor for practical column longevity, particularly in the context of bioprocessing. Many bioprocessing procedures necessitate some form of clean-in-place (CIP) to eliminate contaminants during analytical separations.[56] Given the strong

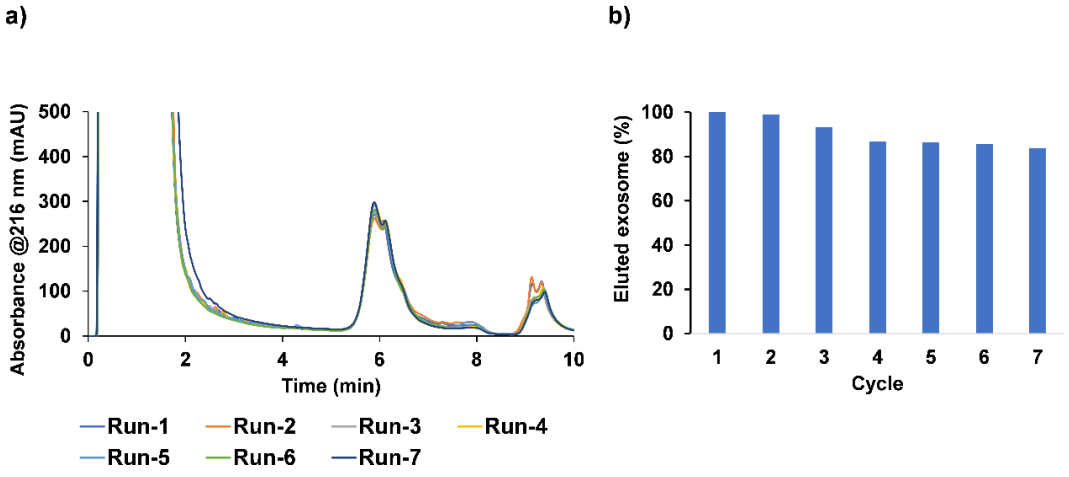

Fig. 3.6 Relative amounts of eluted exosomes for chromatographic cycles a) 7 repetitions employing the column washing step and b) resulting recoveries of exosomes as a function of the first injection response. 100 µL urine was injected with a flow rate of 0.5 mL min^{-1}.

interaction between exosomes and the column surface, addressing carryover becomes a natural area of concern. Existing literature highlights the challenge of removing on-column biological impurities, especially when utilizing pure organic solvents such as ACN or methanol.[57, 58] The PET fiber column exhibits remarkable stability and reproducibility in the HIC mode, particularly when incorporating a thorough washing protocol. To enhance this stability, an inter-injection wash buffer consisting of 90% ACN in PBS was introduced for 5 min. Figure 6a illustrates seven successive chromatographic cycles of a freshly packed new column, each including a washing step, highlighting the efficacy of the wash buffer in maintaining column performance across multiple cycles. The corresponding exosome recoveries from each cycle are depicted in Fig. 6b, revealing that the recovery for the seventh cycle is 83.7% of that observed in the first cycle. The variability in EV elution peak area across the seven replicates is minimal, at 6.85% RSD. Such a high level of repeatability is crucial for future endeavors involving the realm of clinical diagnostics or bioprocessing.

3.4 Conclusions

This study presents a novel HIC-based HPLC method, utilizing Tween-20, for the isolation of exosomes from human urine employing PET C-CP fiber columns. The implementation of a step gradient enabled rapid processing within 10 minutes, yielding high-purity separations with remarkable removal of background proteins (~99%). Notably, the procedure integrates purification, quantification, and size characterization into a single operation, utilizing a HIC chromatographic method on a standard HPLC platform with an in-line MALS detector. TEM micrographs confirmed the structural integrity of the isolated exosomes, although further investigations are necessary to fully validate the vesicular

integrity of the Tween-20 based isolations. The method demonstrates reproducibility across multiple chromatographic cycles, while the low-cost PET C-CP fiber (<< $1 per column) offers significant benefits in terms of material cost (< $50 per liter bed volume) and process throughput compared to commercial HIC column bed materials ($3000 per liter bed volume).[59]

While Tween-20 at its lower concentration (0.1% v/v utilized in this study) shows promise in avoiding membrane disruption of exosomes, optimizing elution strength remains crucial for achieving high recoveries of structurally intact vesicles. Future efforts will be directed towards evaluating Tween-20 elution strength to ensure the maintenance of both structural and biological integrity in high-throughput separations. A comprehensive characterization of the Tween-20 solvent regarding its suitability for genomics and vector applications is also warranted. Despite these considerations, the method offers distinct advantages in various automation aspects of commercial HPLC technologies, including auto-sampling, complete cycle programming, in-line detection and characterization (absorbance and MALS), and fraction collection.

Moreover, in the HIC isolation protocol, solvent choice is a critical factor in the storage of EVs, with Tween-20 emerging as a protective storage solvent that enhances preservation.[60] The isolation and quantification of EVs from a key biomatrix human urine holds significant promise for diverse clinical and biochemical applications. As a milder detergent-based solvent, Tween-20 holds potential for process scale-up, serving as a valuable tool for harvesting large quantities of EVs for therapeutic applications.

3.5 Acknowledgements

This project was supported in part by National Science Foundation grant CHE-2107882 and the National Institutes of Health grant 1RO1GM141347-01A1.

3.6 References

(1) Shao, H.; Im, H.; Castro, C. M.; Breakefield, X.; Weissleder, R.; Lee, H. New technologies for analysis of extracellular vesicles. *Chem. Rev.* **2018**, *118* (4), 1917-1950.

(2) Raposo, G.; Stoorvogel, W. Extracellular vesicles: exosomes, microvesicles, and friends. *J. Cell Bio.* **2013**, *200* (4), 373-383.

(3) H. Rashed, M.; Bayraktar, E.; K. Helal, G.; Abd-Ellah, M. F.; Amero, P.; Chavez-Reyes, A.; Rodriguez-Aguayo, C. Exosomes: from garbage bins to promising therapeutic targets. *Int. J. Mol Sci.* **2017**, *18* (3), 538.

(4) Liu, Y.; Wang, C.; Wei, M.; Yang, G.; Yuan, L. Multifaceted roles of adipose tissue-derived exosomes in physiological and pathological conditions. *Fronti. Physiol.* **2021**, *12*, 669429.

(5) Logozzi, M.; Mizzoni, D.; Di Raimo, R.; Fais, S. Exosomes: a source for new and old biomarkers in cancer. *Cancers* **2020**, *12* (9), 2566.

(6) Ohno, S.-i.; Ishikawa, A.; Kuroda, M. Roles of exosomes and microvesicles in disease pathogenesis. *Adv. Drug Deliv. Rev.* **2013**, *65* (3), 398-401.

(7) Melo, S. A.; Sugimoto, H.; O'Connell, J. T.; Kato, N.; Villanueva, A.; Vidal, A.; Qiu, L.; Vitkin, E.; Perelman, L. T.; Melo, C. A. Cancer exosomes perform cell-independent microRNA biogenesis and promote tumorigenesis. *Cancer Cell* **2014**, *26* (5), 707-721.

(8) Kourembanas, S. Exosomes: Vehicles of Intercellular Signaling, Biomarkers, and Vectors of Cell Therapy. *Annu. Rev. Physiol.* **2015**, *77* (1), 13-27.

(9) Jiang, L.; Gu, Y.; Du, Y.; Liu, J. Exosomes: diagnostic biomarkers and therapeutic delivery vehicles for cancer. *Mol. Pharm.* **2019**, *16* (8), 3333-3349.

(10) Sandfeld-Paulsen, B.; Jakobsen, K. R.; Bæk, R.; Folkersen, B. H.; Rasmussen, T. R.; Meldgaard, P.; Varming, K.; Jørgensen, M. M.; Sorensen, B. S. Exosomal proteins as diagnostic biomarkers in lung cancer. *J. Thorac. Oncol.* **2016**, *11* (10), 1701-1710.

(11) Burke, J.; Kolhe, R.; Hunter, M.; Isales, C.; Hamrick, M.; Fulzele, S. Stem cell-derived exosomes: a potential alternative therapeutic agent in orthopaedics. *Stem Cells Int.* **2016**, *2016*.

(12) Gupta, S.; Rawat, S.; Arora, V.; Kottarath, S. K.; Dinda, A. K.; Vaishnav, P. K.; Nayak, B.; Mohanty, S. An improvised one-step sucrose cushion ultracentrifugation method for exosome isolation from culture supernatants of mesenchymal stem cells. *Stem Cell Res. Ther.* **2018**, *9*, 1-11.

(13) Grigor'Eva, A.; Dyrkheeva, N.; Bryzgunova, O.; Tamkovich, S.; Chelobanov, B.; Ryabchikova, E. Contamination of exosome preparations, isolated from biological fluids. *Biochemistry-Moscow Suppl. Series B: Biomed. Chem.* **2017**, *11*, 265-271.

(14) Taylor, D. D.; Shah, S. Methods of isolating extracellular vesicles impact down-stream analyses of their cargoes. *Methods* **2015**, *87*, 3-10.

(15) Koh, Y. Q.; Almughlliq, F. B.; Vaswani, K.; Peiris, H. N.; Mitchell, M. D. Exosome enrichment by ultracentrifugation and size exclusion chromatography. *Front. Biosci.* **2018**, *23* (3), 865-874.

(16) Hong, C. S.; Muller, L.; Boyiadzis, M.; Whiteside, T. L. Isolation and characterization of CD34+ blast-derived exosomes in acute myeloid leukemia. *PloS One* **2014**, *9* (8), e103310.

(17) Boriachek, K.; Islam, M. N.; Möller, A.; Salomon, C.; Nguyen, N. T.; Hossain, M. S. A.; Yamauchi, Y.; Shiddiky, M. J. Biological functions and current advances in isolation and detection strategies for exosome nanovesicles. *Small* **2018**, *14* (6), 1702153.

(18) Bruce, T. F.; Slonecki, T. J.; Wang, L.; Huang, S.; Powell, R. R.; Marcus, R. K. Exosome isolation and purification via hydrophobic interaction chromatography using a polyester, capillary-channeled polymer fiber phase. *Electrophoresis* **2019**, *40* (4), 571-581.

(19) Wang, L.; Bruce, T. F.; Huang, S.; Marcus, R. K. Isolation and quantitation of exosomes isolated from human plasma via hydrophobic interaction chromatography using a polyester, capillary-channeled polymer fiber phase. *Anal. Chim. Acta* **2019**, *1082*, 186-193.

(20) Huang, S.; Ji, X.; Jackson, K. K.; Lubman, D. M.; Ard, M. B.; Bruce, T. F.; Marcus, R. K. Rapid separation of blood plasma exosomes from low-density lipoproteins via a hydrophobic interaction chromatography method on a polyester capillary-channeled polymer fiber phase. *Anal. Chim. Acta* **2021**, *1167*, 338578.

(21) Jackson, K. K.; Powell, R. R.; Bruce, T. F.; Marcus, R. K. Rapid isolation of extracellular vesicles from diverse biofluid matrices via capillary-channeled polymer fiber solid-phase extraction micropipette tips. *Analyst* **2021**, *146* (13), 4314-4325.

(22) Lal, A.; Pike, J. F. W.; Polley, E. L.; Huang, S.; Sanni, M.; Hailat, T.; Zimmerman, S.; Clay-Gilmour, A.; Bruce, T. F.; Marcus, K. R. Comparison of RNA content from hydrophobic interaction chromatography-isolated seminal plasma exosomes from intrauterine insemination (IUI) pregnancies. *Andrologia* **2022**, *54* (2), e14325.

(23) Huang, S.; Wang, L.; Bruce, T. F.; Marcus, R. K. Evaluation of exosome loading characteristics in their purification via a glycerol-assisted hydrophobic interaction chromatography method on a polyester, capillary-channeled polymer fiber phase. *Biotechnol. Prog.* **2020**, *36* (5), e2998.

(24) Wang, Z.; Marcus, R. K. Determination of pore size distributions in capillary-channeled polymer fiber stationary phases by inverse size-exclusion chromatography and implications for fast protein separations. *J. Chromatogr. A* **2014**, *1351*, 82-89.

(25) Jackson, K. K.; Mata, C.; Marcus, R. K. A rapid capillary-channeled polymer (C-CP) fiber spin-down tip approach for the isolation of plant-derived extracellular vesicles (PDEVs) from 20 common fruit and vegetable sources. *Talanta* **2023**, *252*, 123779.

(26) Jackson, K. K.; Powell, R. R.; Marcus, R. K.; Bruce, T. F. Comparison of the capillary-channeled polymer (C-CP) fiber spin-down tip approach to traditional methods for the isolation of extracellular vesicles from human urine. *Anal. Bioanal. Chem.* **2022**, *414* (13), 3813-3825.

(27) Jackson, K. K.; Marcus, R. K. Rapid isolation and quantification of extracellular vesicles from suspension-adapted human embryonic kidney cells using capillary-channeled polymer fiber spin-down tips. *Electrophoresis* **2023**, *44* (1-2), 190-202.

(28) Ji, X.; Huang, S.; Bruce, T. F.; Tan, Z.; Wang, D.; Zhu, Z.; Marcus, R. K.; Lubman, D. M. A Novel Method of High-Purity Extracellular Vesicle Enrichment from Microliter-scale Human Serum for Proteomic Analysis. *Electrophoresis* **2021**, *42*, 245-256.

(29) Vagenende, V.; Yap, M. G.; Trout, B. L. Mechanisms of protein stabilization and prevention of protein aggregation by glycerol. *Biochemistry* **2009**, *48* (46), 11084-11096.
(30) Osteikoetxea, X.; Sódar, B.; Németh, A.; Szabó-Taylor, K.; Pálóczi, K.; Vukman, K. V.; Tamási, V.; Balogh, A.; Kittel, Á.; Pállinger, É. Differential detergent sensitivity of extracellular vesicle subpopulations. *Org. Biomol. Chem.* **2015**, *13* (38), 9775-9782.

(31) György, B.; Módos, K.; Pállinger, E.; Pálóczi, K.; Pásztói, M.; Misják, P.; Deli, M. A.; Sipos, A.; Szalai, A.; Voszka, I. Detection and isolation of cell-derived microparticles are compromised by protein complexes resulting from shared biophysical parameters. *Blood* **2011**, *117* (4), e39-e48.

(32) Seddon, A. M.; Curnow, P.; Booth, P. J. Membrane proteins, lipids and detergents: not just a soap opera. *BBA-Biomembranes* **2004**, *1666* (1-2), 105-117.

(33) Heller, N. C.; Garrett, A. M.; Merkley, E. D.; Cendrowski, S. R.; Melville, A. M.; Arce, J. S.; Jenson, S. C.; Wahl, K. L.; Jarman, K. H. Probabilistic limit of detection for ricin identification using a shotgun proteomics assay. *Anal. Chem.* **2019**, *91* (19), 12399-12406.

(34) Cvjetkovic, A.; Lötvall, J.; Lässer, C. The influence of rotor type and centrifugation time on the yield and purity of extracellular vesicles. *J. Extracell. Vesicles* **2014**, *3* (1), 23111.

(35) Wysor, S. K.; Marcus, R. K. In-line Coupling of Capillary-Channeled Polymer Fiber Columns with Optical Absorbance and Multi-angle Light Scattering Detection for the Isolation and Characterization of Exosomes. *Anal. Bioanal. Chem.* **2024**, *submitted for publication*.

(36) Gardiner, C.; Shaw, M.; Hole, P.; Smith, J.; Tannetta, D.; Redman, C. W.; Sargent, I. L. Measurement of refractive index by nanoparticle tracking analysis reveals heterogeneity in extracellular vesicles. *J. Extracell. Vesicles* **2014**, *3* (1), 25361.

(37) Randunu, K. M.; Marcus, R. K. Microbore polypropylene capillary channeled polymer (C-CP) fiber columns for rapid reversed-phase HPLC of proteins. *Anal. Bioanal. Chem.* **2012**, *404*, 721-729.

(38) Wang, L.; Marcus, R. K. Evaluation of protein separations based on hydrophobic interaction chromatography using polyethylene terephthalate capillary-channeled polymer (C-CP) fiber phases. *J. Chromatogr. A* **2019**, *1585*, 161-171.

(39) Huang, S.; Wang, L.; Bruce, T. F.; Marcus, R. K. Isolation and quantification of human urinary exosomes by hydrophobic interaction chromatography on a polyester capillary-channeled polymer fiber stationary phase. *Anal. Bioanal. Chem.* **2019**, *411*, 6591-6601.

(40) Witwer, K. W.; Buzás, E. I.; Bemis, L. T.; Bora, A.; Lässer, C.; Lötvall, J.; Nolte-‘t Hoen, E. N.; Piper, M. G.; Sivaraman, S.; Skog, J. Standardization of sample collection, isolation and analysis methods in extracellular vesicle research. *J. Extracell. Vesicles* **2013**, *2* (1), 20360.

(41) Webber, J.; Clayton, A. How pure are your vesicles? *J. Extracell. Vesicles* **2013**, *2* (1), 19861.

(42) Lichtenberg, D. Characterization of the solubilization of lipid bilayers by surfactants. *BBA-Biomembranes* **1985**, *821* (3), 470-478.

(43) Lichtenberg, D.; Ahyayauch, H.; Goñi, F. M. The mechanism of detergent solubilization of lipid bilayers. *Biophys. J.* **2013**, *105* (2), 289-299.

(44) Hjertén, S.; Johansson, K.-E. Selective solubilization with Tween 20 of membrane proteins from Acholeplasma laidlawii. *BBA-Biomembranes* **1972**, *288* (2), 312-325.

(45) Bagrov, D.; Senkovenko, A.; Nikishin, I.; Skryabin, G.; Kopnin, P.; Tchevkina, E. Application of AFM, TEM, and NTA for characterization of exosomes produced by placenta-derived mesenchymal cells. In *J. Phys. Conf. Ser.*, 2021; IOP Publishing: Vol. 1942, p 012013.

(46) Théry, C.; Witwer, K. W.; Aikawa, E.; Alcaraz, M. J.; Anderson, J. D.; Andriantsitohaina, R.; Antoniou, A.; Arab, T.; Archer, F.; Atkin-Smith, G. K. Minimal information for studies of extracellular vesicles 2018 (MISEV2018): a position statement of the International Society for Extracellular Vesicles and update of the MISEV2014 guidelines. *J. Extracell. Vesicles* **2018**, *7* (1), 1535750.

(47) Chia, B. S.; Low, Y. P.; Wang, Q.; Li, P.; Gao, Z. Advances in exosome quantification techniques. *TrAC-Trends Anal. Chem.* **2017**, *86*, 93-106.

(48) Sitar, S.; Kejžar, A.; Pahovnik, D.; Kogej, K.; Tušek-Žnidarič, M.; Lenassi, M.; Žagar, E. Size characterization and quantification of exosomes by asymmetrical-flow field-flow fractionation. *Anal. Chem.* **2015**, *87* (18), 9225-9233.

(49) Ding, M.; Wang, C.; Lu, X.; Zhang, C.; Zhou, Z.; Chen, X.; Zhang, C.-Y.; Zen, K.; Zhang, C. Comparison of commercial exosome isolation kits for circulating exosomal microRNA profiling. *Anal. Bioanal. Chem.* **2018**, *410*, 3805-3814.

(50) Nelson, D. M.; Marcus, R. K. Potential for Ultrafast Protein Separations with Capillary-Channeled Polymer (C-CP) Fiber Columns. *Protein Peptide Letts.* **2006**, *13* (1), 95-99.

(51) Randunu, J. M.; Dimartino, S.; Marcus, R. K. Dynamic Evaluation of Polypropylene Capillary-Channeled Fibers as a Stationary Phase in High Performance Liquid Chromatography. *J. Sep. Sci.* **2012**, *35*, 3270-3280.

(52) Wang, Z.; Marcus, R. K. Roles of Interstitial Fraction and Load Linear Velocity on the Dynamic Biding Capacity of Proteins on Capillary Channeled Polymer Fiber Columns. *Biotechnol. Progr.* **2015**, *15*, 97-109.

(53) Wang, L.; Bruce, T. F.; Huang, S.; Marcus, R. K. Isolation and quantitation of exosomes isolated from human plasma via hydrophobic interaction chromatography using a polyester, capillary-channeled polymer fiber phase *Anal. Chim. Acta* **2019**, *1082*, 186-193.

(54) Huang, S.; Wang, L.; Bruce, T. F.; Marcus, R. K. Evaluation of Exosome Loading Characteristics in their Purification via a Glycerol-Assisted Hydrophobic Interaction Chromatography Method on a Polyester, Capillary-Channeled Polymer Fiber Phase. *Biotechnol. Prog.* **2020**, *36*, e2998.

(55) Billotto, L. S.; Jackson, K. K.; Marcus, R. K. Determination of the Loading Capacity and Recovery of Extracellular Vesicles Derived from Human Embryonic Kidney Cells and Urine Matrices on Capillary-Channeled Polymer (C-CP) Fiber Columns. *Separations* **2022**, *9* (9), 251-264.

(56) Schadock-Hewitt, A. J.; Marcus, R. K. Initial evaluation of protein A modified capillary-channeled polymer fibers for the capture and recovery of immunoglobulin G. *J. Sep. Sci.* **2014**, *37* (5), 495-504.

(57) Bhardwaj, S.; Day, R. Trifluoroethanol removes bound proteins from reversed-phase columns. *LC GC* **1999**, *17* (4), 354-356.

(58) Majors, R. E. The cleaning and regeneration of reversed-phase HPLC columns. *LC GC* **2003**, *21* (1), 19-27.

(59) McCormick, D. Artificial distinctions: Protein A mimetic ligands for bioprocess separations. *Pharm. Technol.* **2005**, *29* (9), 58.

(60) Van De Wakker, S.; Van Oudheusden, J.; Mol, E.; Roefs, M.; Zheng, W.; Görgens, A.; El Andaloussi, S.; Sluijter, J.; Vader, P. Influence of short term storage conditions, concentration methods and excipients on extracellular vesicle recovery and function. *Eur. J. Pharm. Biopharm.* **2022**, *170*, 59-69.

CHAPTER FOUR

SUMMARY AND FUTURE WORK

The work described in Chapter Two demonstrates the potential of PP C-CP fiber surfaces as a promising support phase for SAV immobilization and subsequent capture of biotinylated target proteins. SAV-modified fiber columns were prepared by loading SAV onto the bare fiber surface for 3 min. The investigation into the effect of flow rate and variation of Tween-20 concentrations in PBS loading solvent buffer provided insights into optimizing the binding strategy for enhanced selectivity and reduced non-specific binding. The results demonstrate that the capture efficiency of b-GFP remains unaffected under optimized loading conditions, even in the presence of background-interacting protein mixtures. However, further optimization is warranted to reduce non-specific background protein interactions.

In future research, the project will aim to address the practical challenges associated with capturing biotinylated proteins and antibodies from complex media, particularly by exploring the utilization of protein L on the SAV-modified fiber surfaces. Additionally, efforts will be directed towards adapting the SAV-modified C-CP columns into a tip format, enabling integration into automated sample manipulation platforms and facilitating coupling to 96-well processing formats.

The work presented in Chapter Three develops a new HIC-based HPLC method utilizing Tween-20 for exosome isolation from human urine using PET C-CP fiber columns. By employing a step gradient, the process achieves rapid isolation of exosomes in < 10 min. Notably, the method combines purification, quantification, and size characterization of

exosomes into a single operation, utilizing HIC chromatography on a standard HPLC platform with an in-line MALS detector.

Future work will focus on optimizing the elution strength of Tween-20, to ensure the preservation of structural integrity and biological activity of the eluted exosomes. It is essential to optimize a balance between the extent of potential membrane disruption and achieving high recovery of intact vesicles. Additionally, a comprehensive comparison of Tween-20 solvent with organic modifiers (ACN and glycerol) in HIC-based C-CP methodology will be conducted, aiming to identify the optimal elution solvent for specific end-applications, thereby enhancing the efficacy and versatility of exosome isolation methodologies.

APPENDICES

APPENDIX A

SUPPLEMENTARY MATERIAL FOR CHAPTER TWO

Stability of immobilized SAV on PP fiber upon addition of Tween-20 buffer –

A loading step involving the application of 0.5 mg mL^{-1} SAV onto the PP fiber was executed over a 3-minute period, resulting in a saturated SAV-modified fiber surface. The loading step was followed by a 10-minute washing step with PBS. Subsequently, a 5-minute SAV elution step employing a 40% (v/v) acetonitrile (ACN) solution in PBS was implemented, as depicted in Fig. A1. To evaluate the stability of SAV towards the introduction of Tween-20 at concentrations of 0.5% and 1% to potentially limit non-specific binding, a separate protocol was devised. As illustrated in Fig. A2, the SAV loading step was succeeded by a 10-minute Tween-20 exposure, followed by a 5-minute PBS wash to reduce the chromatographic signal response to the background level. After these processes, the integrated peak areas from the elution phase were compared and are visually presented in Figure A2. The amount of eluted SAV under the RP solvent conditions was compared and found to be effectively the same, suggesting that no SAV had been lost upon exposure to the Tween-20 solutions.

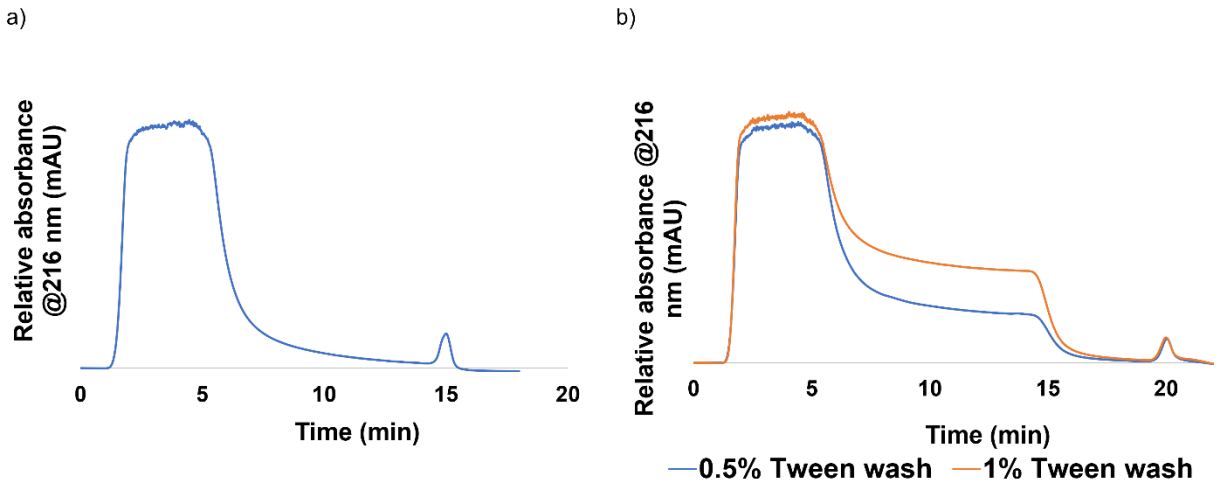

Fig. A1. Response for the 0.5 mg mL^{-1} SAV load and elution with 40% acetonitrile at 0.5 mL min^{-1} flow rate on 10-cm C-CP fiber packed column with the following condition before the elution step, (a) Column washing with PBS for 10 min, and (b) column washing with Tween-20 solution for 10 min followed by 5 min PBS wash.

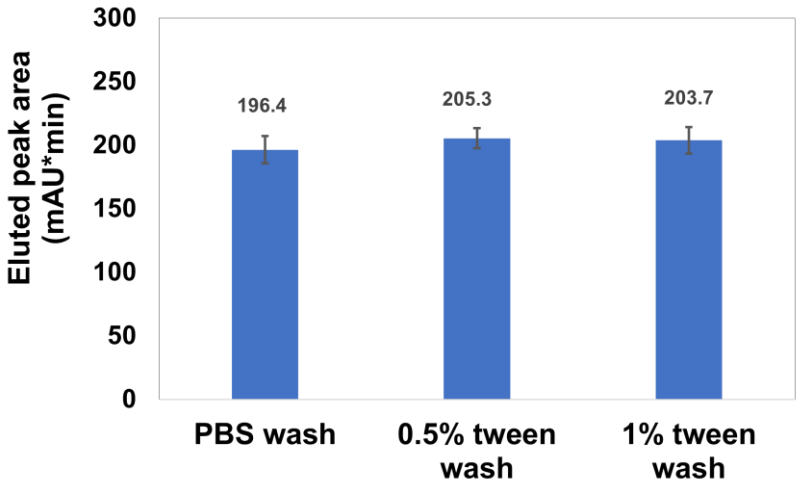

Fig. A2. Comparison of the peak area of SAV elution from the column using 40% acetonitrile at different washing conditions introduced before the elution.